Isatin Derivatives as Inhibitors of Microtubule Assembly

By

Karen L. Beckman

B.S., North Dakota State University, 2005

Submitted to the Department of Medicinal Chemistry and the Faculty of the Graduate School of The University of Kansas in partial fulfillment of the requirements for the degree of Masters of Science.

Thesis Committee:

_____
(Chairperson)

_____

_____

Date defended: _____

The Dissertation Thesis Committee for Karen L. Beckman certifies that this is the approved version of the following dissertation:

Isatin Derivatives as Inhibitors of Microtubule Assembly

Thesis Committee:

_____
(Chairperson)

_____

_____

Date defended: _____

Abstract

This thesis describes the rationale, design, and syntheses of derivatives of isatin (1-H-indole-2,3-dione). Isatin was identified, during a high throughput screen of 10,000 compounds, as a potential scaffold for microtubule-destabilizing agents. Additional screening of purchased isatin derivatives gave rise to four substitution patterns of interest, 7-arylisatins, 5-methyl-*N*-alkyl/aryl isatins, 5-chloro-*N*-alkyl/aryl isatins and 5,7-dichloro-*N*-alkylated isatins. Series of compounds with the substitutions of interest were synthesized to further probe the structure-activity relationship (SAR) of isatin.

The SAR study showed that substitutions in the 5- and 7- positions of the aromatic ring combined with *N*-substitutions increased the disruption of microtubule assembly. The 7-phenylisatin and *N*-arylisatin derivatives were inactive in the biological assay. Several of the 5-chloro-*N*-alkylisatins and the 5,7-dichloro-*N*-alkylisatins were cytotoxic in both MCF-7 and NCI/ADR-RES cell lines. 5,7-Dichloro-*N*-(4-bromobenzyl)isatin was the most active compound against MCF-7 cells, IC_{50} = 2.1 μM. To date the most cytotoxic compound tested is 5-methyl-*N*-(1-propyl)isatin, with an IC_{50} value of 52 nM (microtubule assembly IC_{50} = 2.6 μM) in the drug resistant cancer cell line NCI/ADR-RES.

For my father

Earl L. Beckman

(December 1944 - June 2007)

Acknowledgments

I would like to express my sincere gratitude to my faculty adviser Dr. Gunda I. Georg for her guidance, patience, and support throughout my graduate career. I would like to thank Dr. Richard Himes and his group for performing microtubule assembly and cytotoxicity assays. I would also like to thank Dr. Derek Hook and Dr. Defeng Tian for cytotoxicity studies.

My sincere appreciation is expressed to several faculty members in the Medicinal Chemistry and Chemistry departments and especially to members of my committee; Dr. Brian Blagg, and Dr. Richard Himes.

During my time at KU, I made several friends and I would like to thank Dr. Oliver Hutt, Dr. Jared Spletstoser, Dr. Brandon Turunen, Trinh (Amy) Doan, Melaine Blevins, Christopher Schneider, James McParland, Xingxian (Wayne) Gu, Matthew Leighty, and my Minnesota friends, Susie Emond, and Aaron Teitelbaum. I would especially like to thank my very dear friend Timothy Ribelin for his advise and support. I would also like to thank my family, Joan, Matt, Jenny, and my mother Peggy for their unyielding support and love.

Finally, I would like to thank the National Cancer Institute for providing the MCF-7 and NCI/ADR-RES cell lines, as well as, The Universities of Kansas and Minnesota for financial support.

Table of Contents

List of Figures

List of Tables

Introduction and Background

Microtubules are basic components of cell structure, which take part in a wide number of cellular functions including, cell movement, vesicle transport, and chromosome segregation during mitosis.[1] These functions are performed in conjunction with the dynamic restructuring of the microtubule cytoskeleton, i.e. lengthening and shortening of individual microtubules, tread-milling of microtubules through the cell, or complete disassembly and rebuilding of microtubule arrays.[2]

The dynamic properties of microtubules were apparent to early cytologists, who discovered their importance in the formation of mitotic spindles as early as 1928.[3] Advancements in visualization techniques, such as cryoelectron microscopy, have provided detailed structures of microtubules. The knowledge gained from the structure of microtubules has shed light on the dynamic nature of microtubules.[4]

Microtubules are noncovalent polymers of the protein tubulin. The subunit of a microtubule, a heterodimer of α- and β- tubulin, was first purified using its affinity for the natural product, colchicine.[5] The α- and β- tubulin monomers, are approximately 50% homologous at the amino acid level.[6] The $\alpha\beta$-heterodimers of tubulin polymerize into protofilaments in a head-to-tail association.[7] *In vivo*, 13 protofilaments laterally associate in parallel to form a

hollow, helical microtubule roughly 25 nm wide.[8] The inside of the hollow microtubule is referred to as the lumen. The number of protofilaments associated in a given microtubule is subject to numerous factors, including the isoforms of tubulin involved.[9] The head-to-tail association of αβ -heterodimers gives rise to polarity in the microtubule structure. The faster growing end of the microtubule is referred to as the plus end and the slower growing end is the minus end. The consensus is that in each protofilament the αβ-heterodimers is orientated with β-tubulin exposed at the plus end and α-tubulin exposed at the minus end.[10-12] This polarity is intrinsic to the different polymerization rates at the two ends of the microtubule (**Figure 1**).

Figure 1: Microtubule Structure

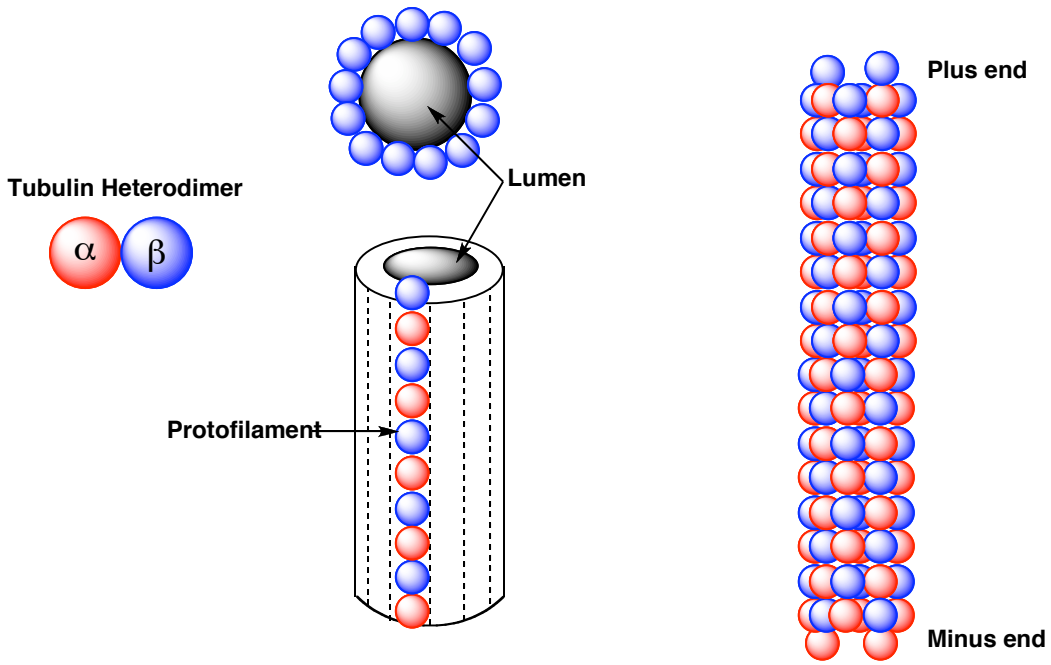

Tubulin heterodimers co-purify with two moles of guanine nucleotide per mole of αβ dimer, with each monomer binding one guanine nucleotide (GTP).[5] α-Tubulin contains a non-exchangeable GTP-binding site known as the N-site. β-Tubulin, in turn, contains an exchangeable GTP-binding site known as the E-site. During polymerization, GTP bound to the E-site is hydrolyzed upon addition of a dimer to the microtubule end, at which point it becomes non-exchangeable.[13]

The biological functions of microtubules in all cells are determined and regulated in large part by their polymerization dynamics. It is important to emphasize that microtubules are not simple equilibrium polymers. Microtubules display two kinds of non-equilibrium dynamics. The first dynamic behavior of microtubules is called 'dynamic instability';[14] the second is called 'tread-milling.'[15]

Dynamic instability is a process in which individual microtubule ends switch between phases of growth and shortening (**Figure 2**).[14] Dynamic instability is characterized by four main variables: the rate of microtubule growth, the rate of shortening, the frequency of transition from the growth or paused state to shortening (this transition is called a 'catastrophe'), and the frequency of transition from shortening to growth or pause (called a 'rescue').[16]

Figure 2: Microtubule Dynamic Instability

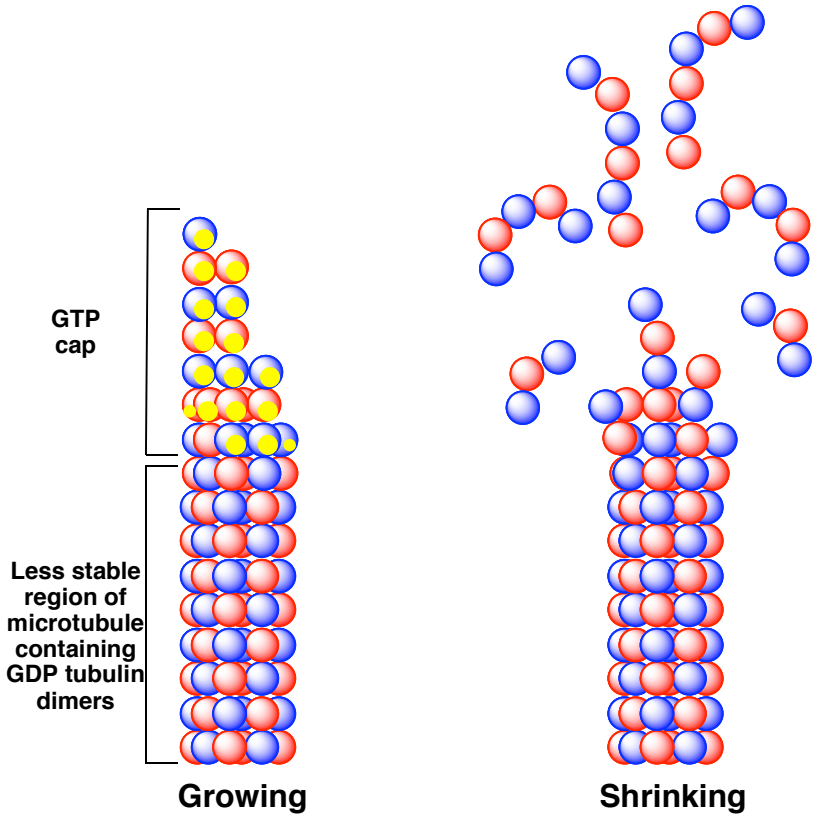

In the polymerization phase, GTP-tubulin subunits add to the end of a microtubule, forming a stabilizing GTP-cap allowing the polymer to grow. During or soon after polymerization, the tubulin subunits hydrolyze their bound GTP and subsequently release the hydrolyzed phosphate. This hydrolysis leads to a conformational change in the αβ-heterodimer, thus destabilizing the polymer. During the depolymerization phase, GDP-tubulin

subunits are released from the microtubule ends at a very rapid rate and subsequently GDP is subsequently exchanged for GTP (**Figure 2 and 3**).

Figure 3: Role of GTP-GDP Exchange in Microtubule Dynamic Instability.

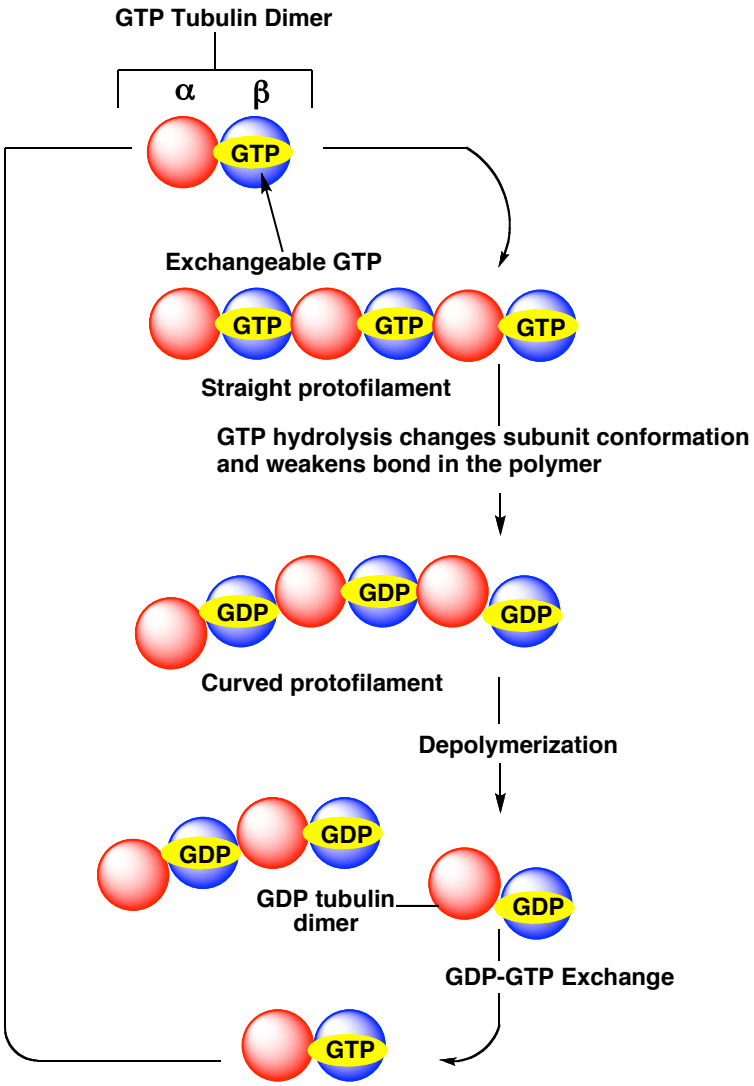

The second dynamic behavior, treadmilling, is a net growth at one microtubule end and balanced net shortening at the opposite end.[15,17] It involves the intrinsic flow of tubulin subunits from the plus end of the microtubule to the minus end and is created by differences in the critical subunit concentration at the opposite microtubule ends. Treadmilling has been implicated as an important phenomenon in mitosis during anaphase chromosome poleward movement.[18]

Compounds that affect microtubule dynamics, and subsequently mitosis, are particularly important in cancer chemotherapy.[19] These agents are considered to be anti-mitotic as they halt the cell cycle at the G2/M-phase interface. **Figure 4** depicts several well-known anti-mitotic agents.

Figure 4: Structures of Anti-mitotic Agents.

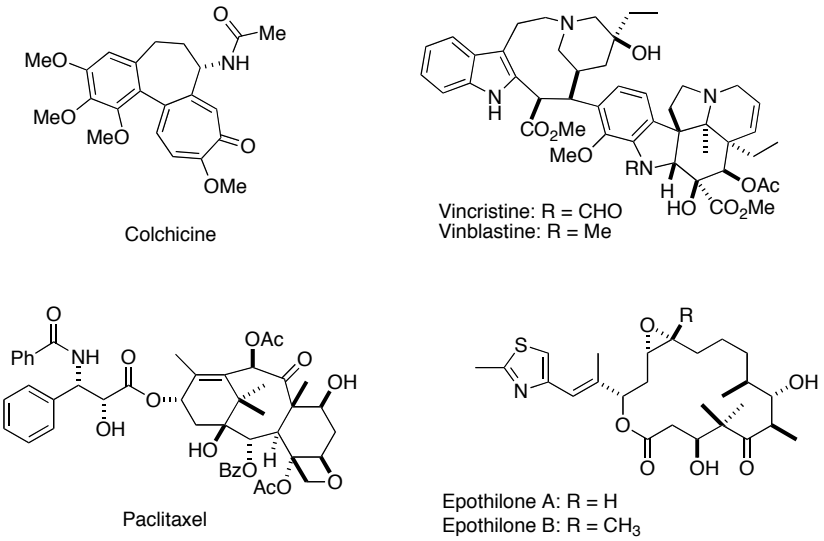

Microtubule anti-mitotic drugs are usually classified into two main groups: microtubule destabilizing and microtubule stabilizing. These drugs can be further classified based on the location of tubulin binding, as depicted in **Table 1**.[20] Tubulin has three distinct binding sites: the taxol, colchicine, and vinblastine domains.

Table 1: Classification of Anti-mitotic Agents

Class	Compounds	Mechanism
1	Paclitaxel, Epothilones, Discodermolide, Eleutherobin	Microtubules hyperassembly and stabilization
2	t-BCEU, T138067, Ottelione	Binding to Cys239
3	Combretastatin A-4, 2-Methoxyestradiol, NSC-639829, Mivobulin	Microtubules destabilization, binding to the colchicine site
4	Maytansine and Rhizoxine (competitive); Macrocyclic polyethers, Peptides, Despipeptides (non-competitive)	Microtubules destabilization, binding to the vinblastine site

The taxol binding pocket is lined by several hydrophobic residues and is situated on the luminal (inside) of the microtubule wall, roughly in the middle of the β monomer.[21] The peeling apart of protofilaments in taxol-stabilized microtubules is greatly inhibited; suggesting the mechanism by which taxol stabilizes microtubules is mainly through strengthening of the

lateral interactions between protofilaments.[22] Other natural products that bind to the taxol binding site are the epothilones,[23] discodermolide,[24] and eleutherobin.[25]

Although not as well defined as the taxol-binding site, the colchicine and vinblastine binding domains primarily interact with the β monomer of tubulin.[26-28] Binding at both of these sites leads to a disruption in microtubule polymerization. Combretastatin A-4[29] and 2-methoxyestradiol[30] are examples of compounds that bind to the colchicine site. Compounds are found to bind in both competitive (maytansine and rhizoxine) and non-competitive (the halichondrins and despipeptides) manners with regard to the vinblastine site.[30]

Current clinically important anti-mitotic agents include, Taxol, Taxotere and the alkaloids vinblastine, and vincristine.[16] Although some of these agents have shown clinical success, they display limitations of drug resistance and undesired side effects due to toxicity of the compounds; therefore, the development of additional microtubule inhibitors is an attractive avenue of exploration. To this end, we conducted a high-throughput screen (HTS) of 10,000 compounds using a fluorescent microtubule assembly assay to identify potential inhibitors of microtubule polymerization.

Microtubule polymerization is typically determined as a measure of turbidity using a spectrophotometer. This method encounters limitations when

a high number of simultaneous determinations are desired. Microtiter plates, used in high throughput systems, have a much smaller path-length than the standard 1 cm absorption cell, and the signal is decreased accordingly.[19] In contrast, the fluorescence signal can be much more sensitive and less prone to interference. 4',6-Diamidino-2-phenylindole (DAPI), **Figure 5**, a DNA interculator, binds to dimeric and polymeric tubulin with differing affinities and thus has been useful in the development of HTS methods for microtubule polymerization.[31]

Figure 5: Structure of DAPI

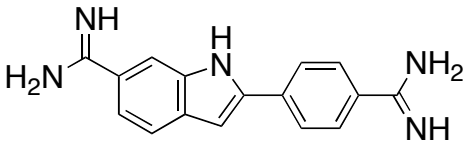

DAPI: 4',6-diamidino-2-phenylindole

Unlike other binders of tubulin, DAPI does not interfere with the binding of taxol or colchicine. Therefore, in the presence of microtubule stabilizing agents, an increase in fluorescence is observed; a decrease in fluorescence is observed in the presence of microtubule destabilizing agents.

The HTS identified sixty compounds displaying an inhibitory activity toward microtubule polymerization. **Table 2** depicts the most active

compounds identified during the HTS. Within these compounds, 60% of the compounds contain the core scaffold isatin (1-H-indole-2, 3-dione); the most active compound being 5-methyl-*N*-(1-propyl)isatin with an IC_{50} value of 52.0 μg/mL.

Table 2: **Most Active High Throughput Screen Compounds**

	Microtubule Assembly		Microtubule Assembly
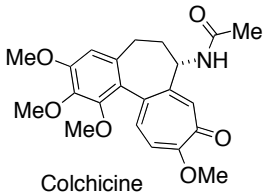 Colchicine	IC_{50} 5 μg/mL	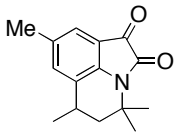	IC_{50} 144 μg/mL
		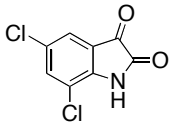	IC_{50} 158 μg/mL
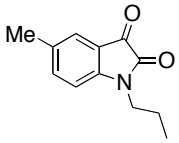	IC_{50} 52.0 μg/mL	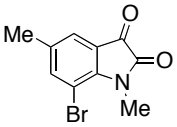	IC_{50} 180 μg/mL
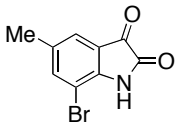	IC_{50} 63.0 μg/mL	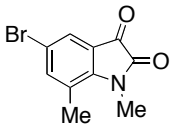	IC_{50} 189 μg/mL
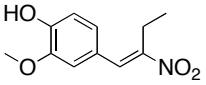	IC_{50} 87 μg/mL	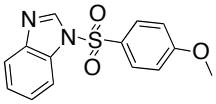	IC_{50} 244 μg/mL
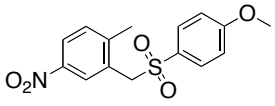	IC_{50} 108 μg/mL	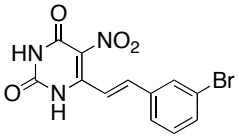	IC_{50} 259 μg/mL

Isatin, a proposed oxidative metabolite of the amino acid tryptophan, (**Figure 6**) was first isolated in 1841 as a product from the oxidation of indigo.[32] In nature, it is found in plants of the genus *Isatis*[33] and *Couroupita guianensis.*[34] A variety of substituted isatins are also found in nature such as the melosatin alkaloids (methoxy phenylpentyl isatins) obtained from the Caribbean tumorigenic plant *Melochia tomentosa*,[35] as well as 6-(3'-methylbuten-2'-yl)isatin isolated from the fungi *Streptomyces albus*.[36]

Figure 6: Origins of Isatin

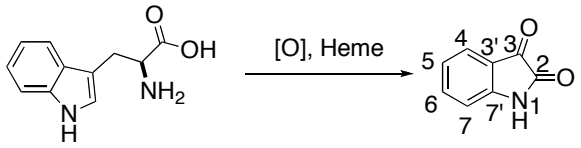

tryptophan isatin

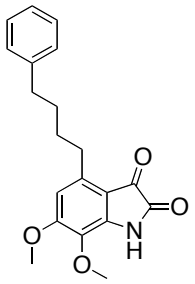

Melosatin A

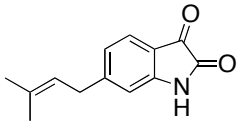

6-(3' -methylbuten-2' -yl)isatin

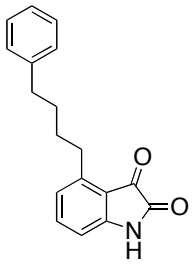

Melosatin B

The most commonly used method for the preparation of isatin is the Sandmeyer procedure (**Scheme 1**).[37]

Scheme 1

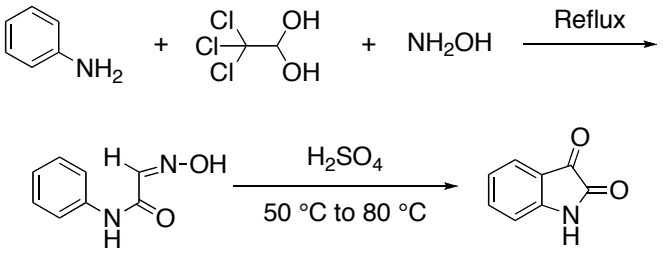

This protocol involves the formation of an isonitrosoacetanilide from chloral-hydrate and aniline, in the presence of hydroxylamine hydrochloride (**Scheme 2**), followed by acid catalyzed cyclization to the isatin.[38]

Scheme 2

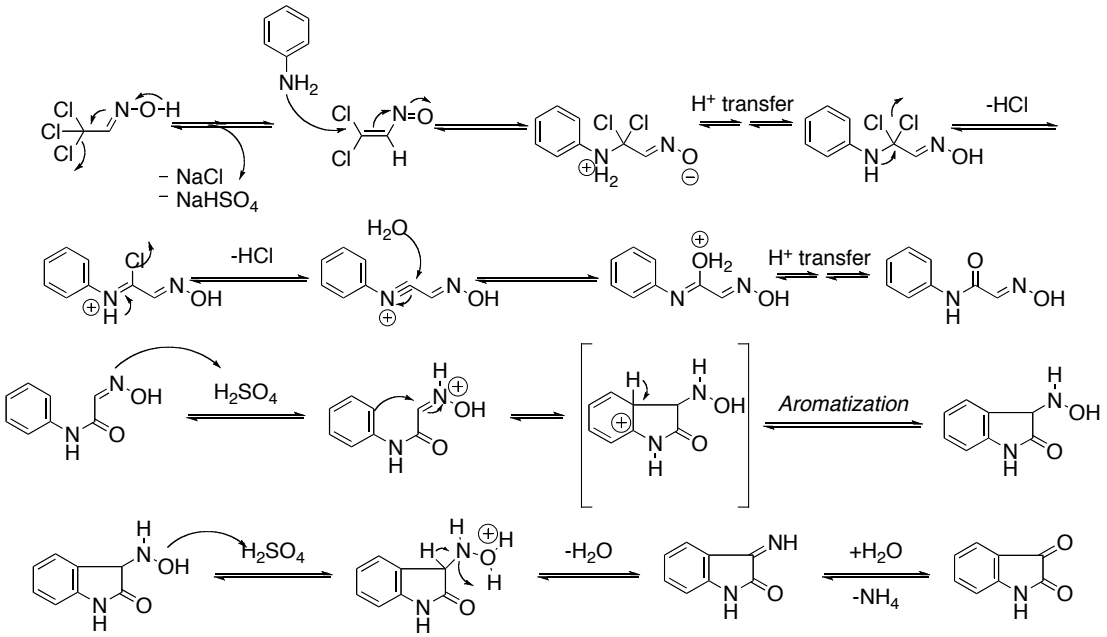

Another frequently used method developed by Stolle[39] involves the treatment of an aniline with oxalyl chloride followed by a Friedel-Crafts-type intramolecular acylation in the presence of a strong Lewis acid (**Scheme 3**).

Scheme 3

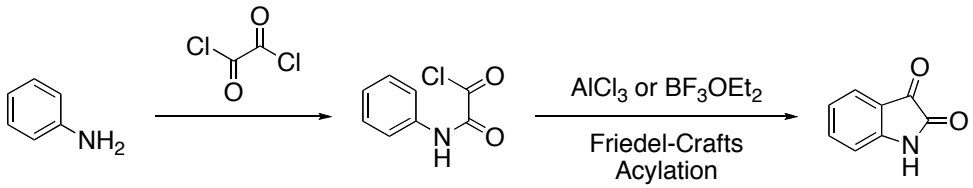

Since both of these methodologies require electrophilic attack on the aromatic ring, the presence of strong electron-withdrawing substitutes tends to inhibit the reaction. The Gassman[40] procedure (**Schemes 4 and 5**) depends on the conversion of anilines into 3-(methylthio)oxindoles followed by oxidative removal of the methylthio group via chlorination and subsequent hydrolysis. The advantage of this procedure is that the method is compatible with the presence of both electron-withdrawing and electron-donating groups.

Scheme 4

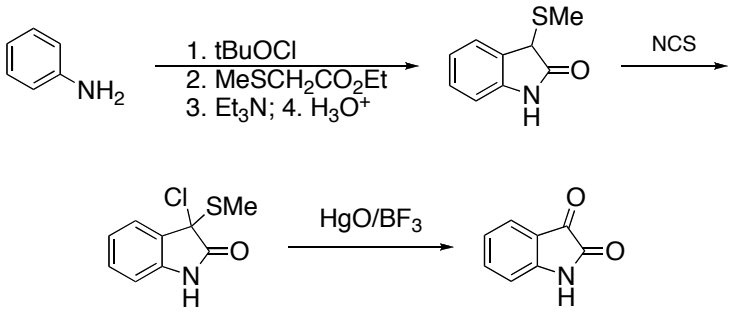

Scheme 5

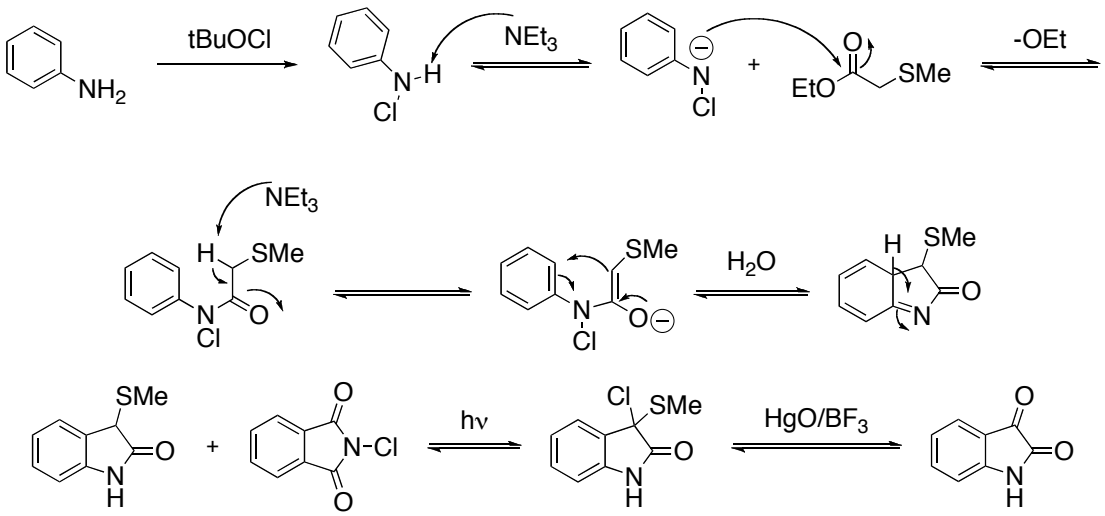

These three common methodologies suffer from the lack of regioselectivity and *meta*-substituted anilines generally give rise to a mixture of 4- and 6- substituted isatins. This problem can be overcome using the directed *ortho*-metalation procedure (**Scheme 6**).[41]Although the directed

ortho-metalation method has advantages, it is not widely used in practice due to the sensitive reaction conditions and expense of the reagents when compared to the other methodologies.

Scheme 6

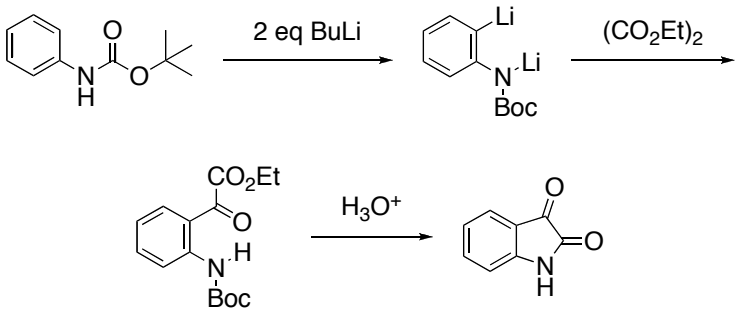

The isatin scaffold proves to be a privileged structure, with many of its derivatives possessing biological activities (**Figure 7**). Isatin displays CNS activity having been identified as an inhibitor of monoamine oxidase B (MAO B)[42] as well as antibacterial and antiproliferative activity.[43] Additional analogs have displayed inhibitory activity against eLF2 kinase activator,[44] TNF-α[45] CDK2,[46] and SARS protease.[47] Schiff bases of the isatin scaffold have anti-small pox[48]and GAL_3 receptor antagonist capabilities.[49] Radio-labeled isatins have also been used to visualize the inhibition of pro-apoptotic enzymes caspase 3 and 7.[50]

Figure 7: Biologically Active Isatins

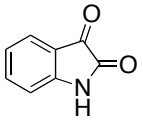

MAO B Inhibitor

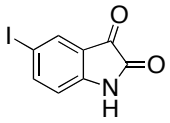

TNF-α Inhibitor (COX-2 and iNOS)

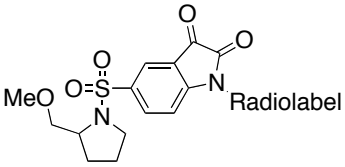

Capase 3 and 7 Inhibitor

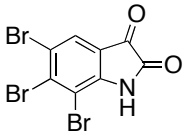

CDK2 Inhibitor

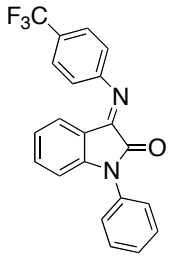

GAL_3 Receptor Antagonist

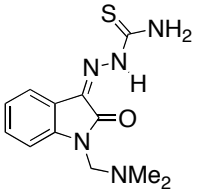

Anti Small Pox

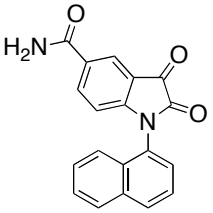

SARS Protease Inhibitor

Results and Discussion

In light of the wealth of biological activity of isatins and the HTS data, we ascertained that isatin would be a valuable lead scaffold upon which a structure-activity relationship (SAR) study could be conducted. To this end, a series of isatin derivatives were purchased from vendors and tested in both the microtubule assembly assay and cytotoxicity assays (cell lines: MCF-7 and NCI/ADR-RES) (**Table 3**).

Table 3: Biological Activity of Purchased Compounds

	Microtubule Assay	MCF-7	NCI/ADR-RES[a]
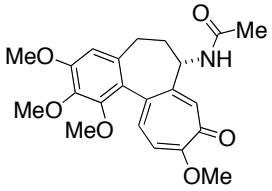	IC_{50} 5.0 μM $IC_{50}/IC_{50(col)}$: 1.0	IC_{50} 0.005 μM	IC_{50} 1 μM
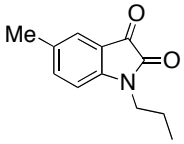	IC_{50} 2.6 μM $IC_{50}/IC_{50(col)}$: 0.5	IC_{50} 9 μM	IC_{50} 0.052 μM
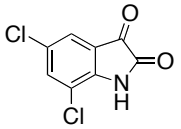	IC_{50} 12.3 μM $IC_{50}/IC_{50(col)}$: 2.5	IC_{50} 6 μM	IC_{50} 6 μM
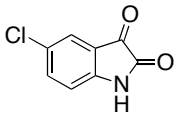	IC_{50} 33 μM $IC_{50}/IC_{50(col)}$: 6.6	IC_{50} 11 μM	IC_{50} 17 μM
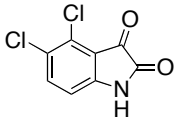	IC_{50} >100 μM $IC_{50}/IC_{50(col)}$: 20	IC_{50} 20 μM	IC_{50} 30 μM
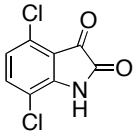	IC_{50} >100 μM $IC_{50}/IC_{50(col)}$: 20	IC_{50} 24 μM	IC_{50} 8 μM
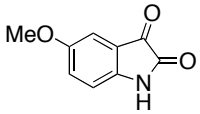	IC_{50} ~100 μM $IC_{50}/IC_{50(col)}$: ~20	IC_{50} 22 μM	IC_{50} 42 μM
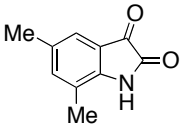	IC_{50} ~100 μM $IC_{50}/IC_{50(col)}$: ~20	IC_{50} >100 μM	IC_{50} >100 μM

[a] NCI/ADR-RES formerly known as MCF7-ADR

The initial biological screens identified four potential lead compounds with promising activity against the drug resistant cancer cell line NCI/ADR-RES (**Scheme 7**).

Scheme 7

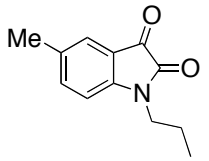

IC_{50} 0.052 μM

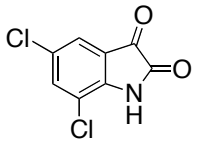

IC_{50} 6 μM

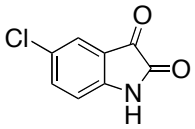

IC_{50} 17 μM

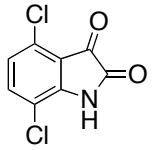

IC_{50} 8 μM

These screens also showed that substitutions in the 5 and 7 positions of the aromatic ring combined with *N*-substitutions increased in activity the microtubule assembly assay. 5-Methyl-*N*-(1-propyl)isatin was the most active compound in this series with an IC_{50} value for NCI/ADR-RES (0.052 μM) in the sub-micromolar range as well as low micromolar IC_{50} values in the MCF-7 cell line and microtubule assembly assay, 9 μM, and 2.6 μM, respectively. Additionally, 5-chloroisatin showed activity in both MCF-7 (IC_{50} 11 μM) and NCI/ADR-RES cell lines (IC_{50} 17 μM); although it was less active in the microtubule assembly assay (IC_{50} 33 μM).

Interestingly, 4,7-dichloroisatin did not inhibit tubulin polymerization but displayed a cytotoxic effect in the low micromolar range making it a potential

lead compound. There are two main synthetic challenges associated with synthesizing 4,7-disubstituted isatins: addition of bulk in the *ortho* positions leading to sluggish ring closure and electron-withdrawing substitutes also leading to sluggish electrophilic attack on the aromatic ring. Further evaluation of the biological data showed that 4,5-dichloroisatin did not affect tubulin polymerization and showed reduced cytotoxicity against NCI/ADR-RES, while the activity of 5,7-dichloroisatin was similar to the 4,7-derivative. Therefore it could be postulated that the cytotoxicity of the 4,7-dichloroisatin is likely the result of substitution in position seven. Based on these evaluations, 4,7-dichloroisatin was removed as a new lead compound in favor of the 7-monosubstituted isatin derivatives. These results suggested four substitution patterns of interest: 7-substituted isatins, 5-alkyl-*N*-alkyl/aryl isatins, 5-chloro-*N*-alkyl/aryl isatins and 5,7-dichloro-*N*-alkylated isatins (**Scheme 8**).

Scheme 8

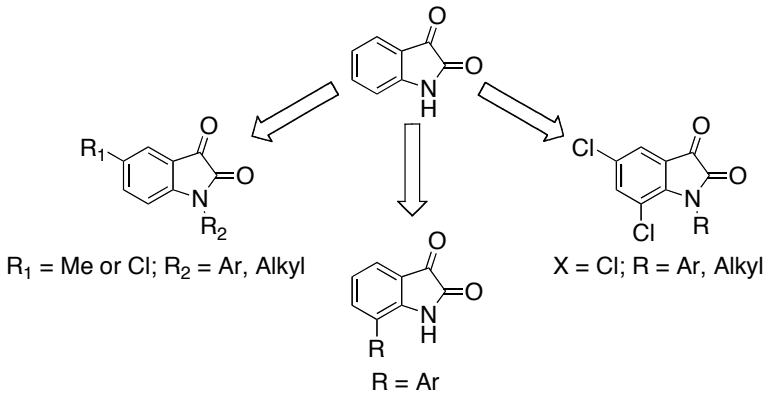

7-Phenylisatins. In order to probe the SAR of the isatin scaffold, a series of 7-aryl substituted isatins were synthesized using a palladium-catalyzed cross-coupling reaction described by Lisowski and coworkers (**Scheme 9**).[51]

Scheme 9

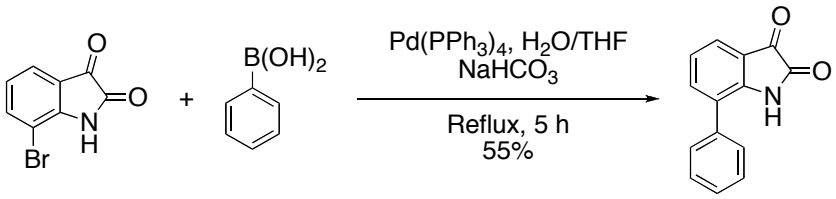

First 2-bromoaniline was reacted under acidic conditions with chloral hydrate in the presence of hydroxylamine hydrochloride and sodium sulfate via the Sandmeyer methodology (**Scheme 10**) to yield an off-white precipitate of isonitrosoacetanilide. This precipitate was filtered and used immediately in the acid catalyzed cyclization, yielding 7-bromoisatin, a bright orange solid.

Scheme 10

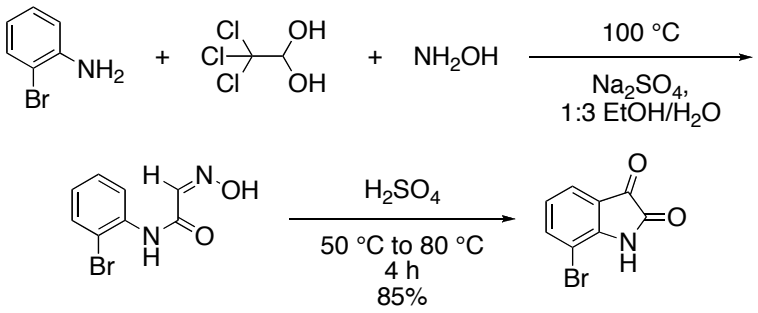

Initial attempts using this 2-step procedure were unsuccessful with yields around 24%. These low yields could be attributed to the precipitation of 2-bromoaniline during initial formation of the isonitrosoacetanilide intermediate. Modification of the Sandmeyer procedure, as suggested by de Silva and coworkers, called for the addition of ethanol to the reaction such that the ratio of ethanol to water is 1:3 (v:v).[52] These modifications produced biphasic reactions and increased reaction yields to 85%.

With the 7-bromoisatin starting material in hand, a series of Suzuki cross-couplings were performed to determine the optimal catalyst system (**Table 4**). Although original work by Lisowski used boronic acids as coupling partners, we opted to use trifluoroborates as coupling agents due to their availability and increased stability under atmospheric conditions.[53]

Table 4: Suzuki Cross-Coupling Optimizations

	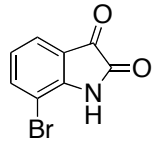	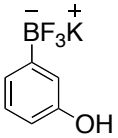	Catalyst System	$NaHCO_3$	Yield
1	0.10 mmol	0.11 mmol	5% $Pd(OAc)_2$, 5% S-PHOS	0.2 mmol	0%
2	0.10 mmol	0.11 mmol	2% $Pd(dppf)_2Cl_2$	0.2 mmol	30%
3	0.10 mmol	0.11 mmol	1% $Pd(PPh_3)_4$	0.2 mmol	66%
4	0.10 mmol	0.11 mmol	2% $Pd(PPh_3)_4$	0.2 mmol	70%
5	0.10 mmol	0.11 mmol	10% $Pd(PPh_3)_4$	0.2 mmol	74%

* Reaction condition: 1:1 THF/H_2O degassed, reflux, 5 h

The catalyst system in reaction **1** of $Pd(OAc)_2$, and S-PHOS[54] was unsuccessful, yielding only starting materials and isatin ring-opened degradation products. Similarly, reaction **2** was plagued by ring-opened degradation. Although the catalyst system of reaction **5,** 10% $Pd(PPh_3)_4$, provided the best yields the expense and air sensitivity of the catalyst led to the selection of catalyst system **4**, 2% $Pd(PPh_3)_4$, for the subsequent Suzuki cross-couplings. The synthetic yields were best for the least hindered substrates, shown in **Table 5**.

Table 5: **Yields and Microtubule Assembly Results of 7-Arylisatins**

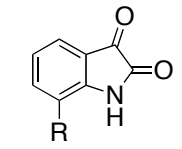

R	Yield IC_{50}	R	Yield IC_{50}
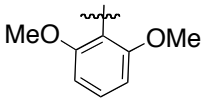	20% >100 μM	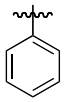	60% >100 μM
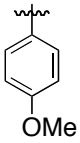	74% >100 μM	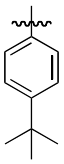	10% >100 μM
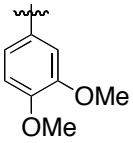	24% >100 μM	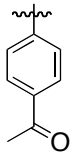	44% >100 μM
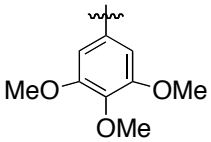	46% >100 μM	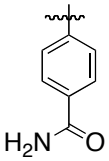	19% >100 μM
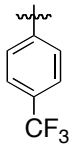	8.9% >100 μM	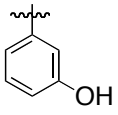	74% >100 μM
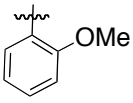	32% >100 μM	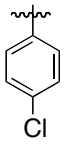	24% >100 μM
	65% >100 μM	Br	85% 31 μM

The only compound showing activity, 7-bromoisatin, which exhibited an IC_{50} value of 31 μM, suggested that substitution in position seven of the isatin ring has little effect on the relative activity of isatin. The increased activity in the lead compounds, 5-methyl-*N*-(1-propyl)isatin and 5,7-dichloroisatin, is a result of substitution in position five of isatin.

The remaining scaffolds to be studied are 5-methylisatin, 5-chloroisatin, and 5,7-dichloroisatin (**Scheme 11**). Three series of *N*-alkylated and *N*-arylated derivatives were synthesized to complete the SAR study.

Scheme 11

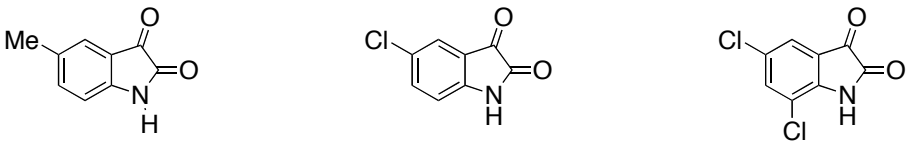

***N*-Alkylated Isatins.** 5-Methylisatin and 5-chloroisatin were both obtained from commercial sources and used without further purification. 5,7-Dichloroisatin was synthesized in a 53% yield via Sandmeyer methodology (**Scheme 12**).

Scheme 12

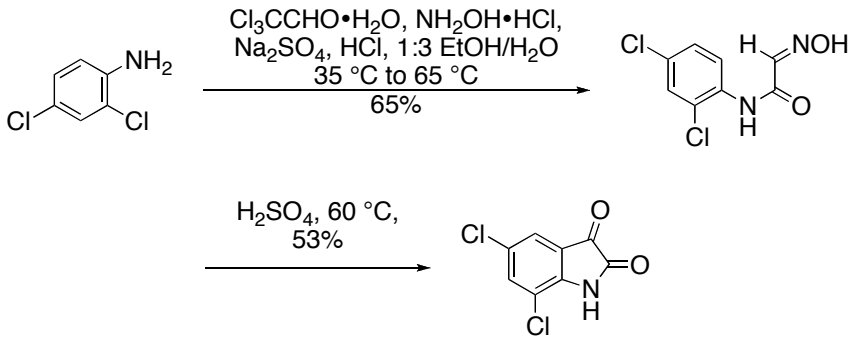

There are several procedures for the *N*-alkylation of isatins described in the literature.[32,55,56] The procedure by Garden and coworkers, was chosen as our standard methodology for *N*-alkylation of isatin (**Scheme 13**).[57]

Scheme 13

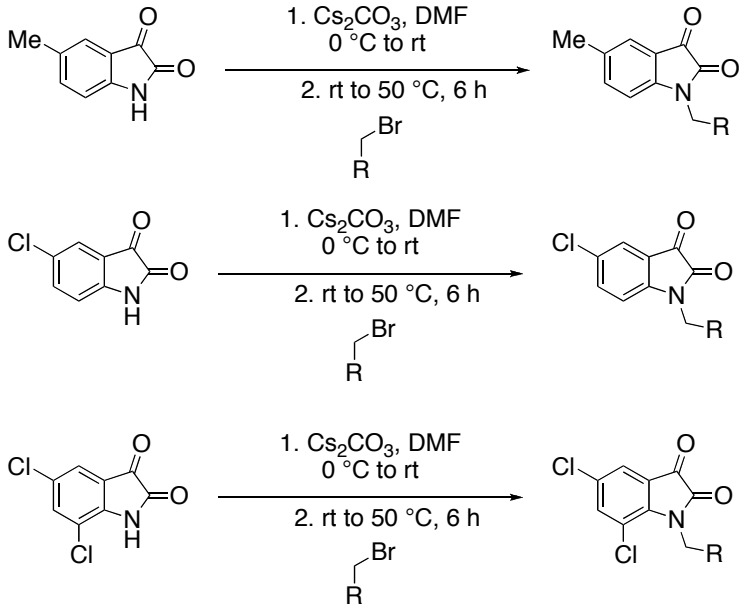

Initially the substituted isatin was dissolved in dry dimethyl formamide (DMF) producing a bright reddish-orange solution. The reaction temperature was reduced to 0 °C. The addition of cesium carbonate rendered the reaction medium a dark purple color. After allowing the reaction to warm to room temperature, the addition of the appropriate alkylating agent led to the return of the reddish-orange color, becoming more vibrant with increased temperature. Yields ranged from 40% to 90% as seen in **Table 6**. Further optimization studies were not conducted. The synthesized compounds were then submitted for biological evaluation (**Table 7, 8 and 9**).

Table 6: *N*-Alkylation Yields

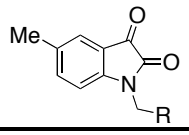	Yield	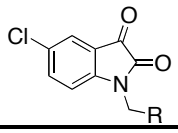	Yield	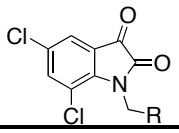	Yield
	83%		65%		36%
	48%		36%		20%
	58%		62%		12%
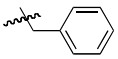	52%	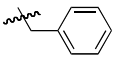	84%	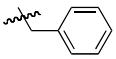	34%
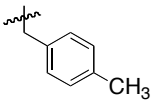	68%	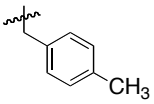	71%	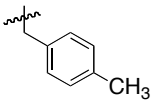	53%
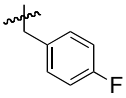	86%	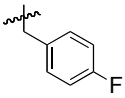	78%	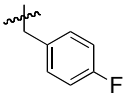	48%
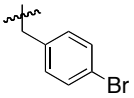	96%	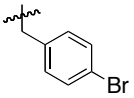	91%	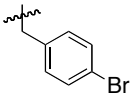	41%
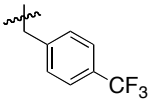	83%	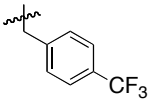	89%	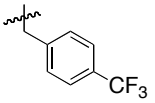	88%
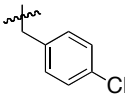	40%	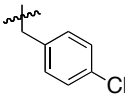	51%	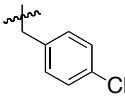	45%

Table 7: Biological Evaluation of 5-Methyl-*N*-Alkylisatins

	Microtubule Assay	MCF-7	NCI/ADR-RES[a]
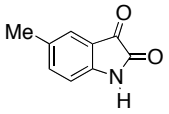	IC_{50} >100 μM $IC_{50}/IC_{50(col)}$: N/A	IC_{50} >100 μM	IC_{50} >100 μM
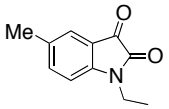	IC_{50} 16 μM $IC_{50}/IC_{50(col)}$: 3.2	IC_{50} >100 μM	IC_{50} >100 μM
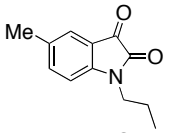	IC_{50} 2.6 μM $IC_{50}/IC_{50(col)}$: 0.5	IC_{50} 9 μM	IC_{50} 0.052 μM
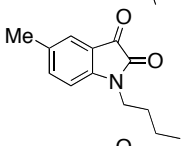	IC_{50} 12.8 μM $IC_{50}/IC_{50(col)}$: 2.6	IC_{50} >100 μM	IC_{50} 5 μM
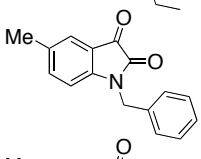	IC_{50} 4 μM $IC_{50}/IC_{50(col)}$: 0.8	IC_{50} >100 μM	IC_{50} >100 μM
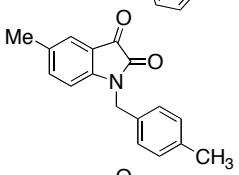	IC_{50} 5.7 μM $IC_{50}/IC_{50(col)}$: 1.1	IC_{50} >100 μM	IC_{50} >100 μM
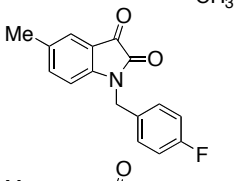	IC_{50} 5.5 μM $IC_{50}/IC_{50(col)}$: 1.1	IC_{50} >100 μM	IC_{50} >100 μM
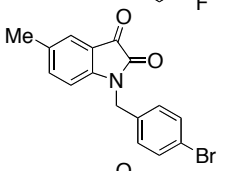	IC_{50} 6.5 μM $IC_{50}/IC_{50(col)}$: 1.3	IC_{50} >100 μM	IC_{50} 31 μM
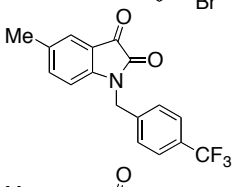	IC_{50} 5 μM $IC_{50}/IC_{50(col)}$: 1.0	IC_{50} >100 μM	IC_{50} 20 μM
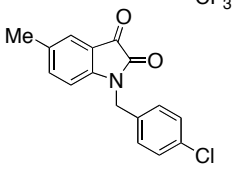	IC_{50} 4 μM $IC_{50}/IC_{50(col)}$: 0.8	IC_{50} >100 μM	IC_{50} 40 μM

[a] NCI/ADR-RES formerly known as MCF7-ADR

[b] IC_{50} values for Colchicine is 5 μM

Table 8: Biological Evaluation of 5-Chloro-*N*-Alkylisatins

	Microtubule Assay[b]	MCF-7	NCI/ADR-RES[a]
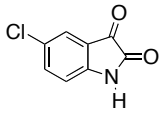	IC_{50} 33 μM $IC_{50}/IC_{50(col)}$: 6.6	IC_{50} 11 μM	IC_{50} 17 μM
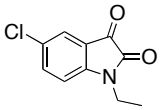	IC_{50} 4.2 μM $IC_{50}/IC_{50(col)}$: 0.8	IC_{50} >100 μM	IC_{50} 7 μM
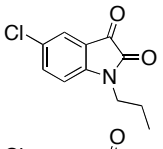	IC_{50} 5.4 μM $IC_{50}/IC_{50(col)}$: 1.1	IC_{50} >100 μM	IC_{50} 6 μM
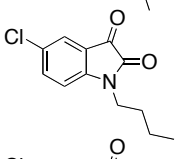	IC_{50} 5.2 μM $IC_{50}/IC_{50(col)}$: 1.0	IC_{50} 31 μM	IC_{50} 12 μM
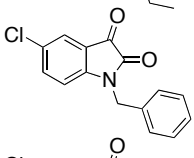	IC_{50} 6.4 μM $IC_{50}/IC_{50(col)}$: 1.3	IC_{50} 81 μM	IC_{50} 19 μM
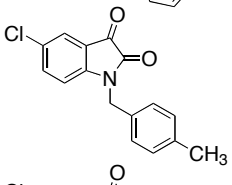	IC_{50} 6.0 μM $IC_{50}/IC_{50(col)}$: 1.2	IC_{50} 5 μM	IC_{50} 8 μM
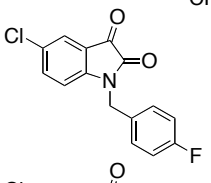	IC_{50} 5 μM $IC_{50}/IC_{50(col)}$: 1.0	IC_{50} >100 μM	IC_{50}17 μM
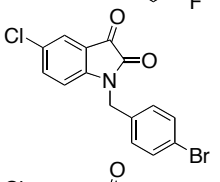	IC_{50} 5 μM $IC_{50}/IC_{50(col)}$: 1.0	IC_{50} 24 μM	IC_{50} 10 μM
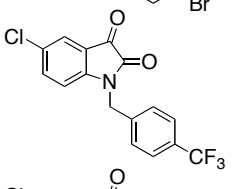	IC_{50} 11.2 μM $IC_{50}/IC_{50(col)}$: 2.2	IC_{50} 63 μM	IC_{50} 17 μM
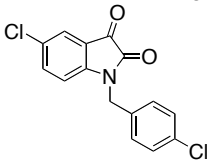	IC_{50} 12.5 μM $IC_{50}/IC_{50(col)}$: 2.5	IC_{50} 14 μM	IC_{50} 8 μM

[a] NCI/ADR-RES formerly known as MCF7-ADR

[b] IC_{50} value of Colchicine is 5 μM

Table 9: Biological Evaluation of 5,7-Dichloro-*N*-Alkylisatins

	Microtubule Assay[b]	MCF-7	NCI/ADR-RES[a]
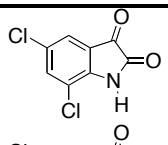	IC_{50} 12.3 μM $IC_{50}/IC_{50(col)}$: 2.5	IC_{50} 6 μM	IC_{50} 6 μM
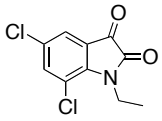	IC_{50} 3.2 μM $IC_{50}/IC_{50(col)}$: 0.64	IC_{50} 18 μM	IC_{50} 7 μM
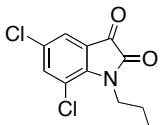	IC_{50} 3.0 μM $IC_{50}/IC_{50(col)}$: 0.6	IC_{50} 13 μM	IC_{50} 3 μM
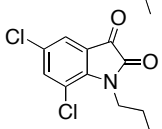	IC_{50} 3.5 μM $IC_{50}/IC_{50(col)}$: 0.7	IC_{50} 6 μM	IC_{50} 1 μM
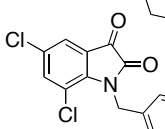	IC_{50} 8 μM $IC_{50}/IC_{50(col)}$: 1.6	IC_{50} 8 μM	IC_{50} 4 μM
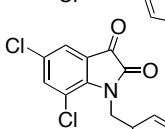	IC_{50} 13 μM $IC_{50}/IC_{50(col)}$: 2.6	IC_{50} 4 μM	IC_{50} 2 μM
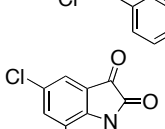	IC_{50} 13 μM $IC_{50}/IC_{50(col)}$: 2.6	IC_{50} 4 μM	IC_{50} 3 μM
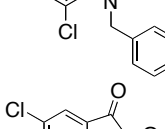	IC_{50} 5.5 μM $IC_{50}/IC_{50(col)}$: 1.1	IC_{50} 2 μM	IC_{50} 2 μM
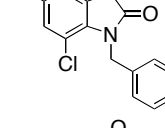	IC_{50} 11.5 μM $IC_{50}/IC_{50(col)}$: 2.3	IC_{50} 19 μM	IC_{50} 7 μM
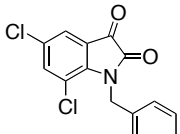	IC_{50} 8.5 μM $IC_{50}/IC_{50(col)}$: 1.7	IC_{50} 40 μM	IC_{50} 7 μM

[a] NCI/ADR-RES formerly known as MCF7-ADR
[b] IC_{50} value for Colchicine is 5 μM

The compounds showed a significant improvement in biological activity when compared to 7-phenylisatins. All of the compounds were active in the microtubule assembly assay with IC_{50} values ranging from 2.6 - 16 μM; reinforcing earlier SAR findings that microtubule assembly activity is improved by nitrogen alkylation and substitution in position five of the isatin core.

Although all of the 5-methylisatin derivatives displayed activity in the microtubule assembly assay, the majority of derivatives lacked substantial cytotoxicity in both MCF-7 and NCI/ADR-RES cell lines. 5-Methyl-*N*-(1-propyl)isatin was the only 5-methylisatin derivative to show activity in MCF-7 cells, IC_{50} 9 μM . This compound was also the most active, of all the compounds synthesized, in both the microtubule assembly assay, IC_{50} = 2.6 μM, and against the NCI/ADR-RES cell line, IC_{50} = 0.052 μM. 5-Methyl-*N*-(1-butyl)isatin also showed activity in NCI/ADR-RES cells with an IC_{50} value of 5 μM.

The 5-chloroisatin derivatives were more active than the 5-methylisatin derivatives in MCF-7 and NCI/ADR-RES cell lines. Similar to the 5-methylisatin derivatives, 5-chloro-*N*-(ethyl)isatin and 5-chloro-*N*-(1-propyl)isatin displayed selective cytotoxic activity for NCI/ADR-RES over MCF-7 cells. The increases in MCF-7 cytotoxicity, for the 5-chloroisatins, are roughly associated with increases in log P of the compounds. The increases in NCI/ADR-RES cytotoxicity are not as closely associated with increases in

log P. The most active compound of the 5-chloroisatin derivatives was 5-chloro-*N*-(4-methylbenzyl)isatin with an IC_{50} value of 6.0 μM in the microtubule assembly assay, and IC_{50} values of 5 μM and 8 μM in MCF-7 and NCI/ADR-RES respectively.

The 5,7-dichloroisatin derivatives were also considerably more cytotoxic than the 5-methylisatins. Similar to the 5-chloroisatins, 5,7-dichloro-*N*-(1-propyl)isatin was active only in the microtubule assembly assay, IC_{50} = 3.0 μM and the NCI/ADR-RES cell line, IC_{50} = 3.0 μM. Several compounds were active against both cell lines as well as in the microtubule assembly assay. The cell line NCI/ADR-RES responded the most to 5,7-dichloro-*N*-(1-butyl)isatin, IC_{50} = 1 μM, similar to the IC_{50} value of colchicine. 5,7-Dichloro-*N*-(1-butyl)isatin was also active in the microtubule assembly assay, IC_{50} = 3.5 μM, and against MCF-7 cells, IC_{50} = 6.4 μM. 5,7-Dichloro-*N*-(4-methylbenzyl)isatin and 5,7-dichloro-*N*-(4-bromobenzyl)isatin were the most active compounds of the 5,7-dichloroisatins; both displayed low micromolar activity in MCF-7 (IC_{50} = 4 μM, IC_{50} = 2.1 μM) and NCI/ADR-RES (IC_{50} = 2 μM and IC_{50} = 2 μM) cell lines.

Of the thirty *N*-alkylated isatin derivatives synthesized, eleven displayed greater activity in the microtubule assembly assay over colchicines; cytotoxicity in MCF-7 cell lines was also increased. Two compounds, 5-

methyl-*N*-(1-propyl)isatin and 5,7-dichloro-*N*-(1-butyl)isatin were more cytotoxic than colchicine in NCI/ADR-RES cells.

***N*-Arylisatins.** The final series of compounds prepared were the *N*-arylisatin derivatives. Initial attempts toward the preparation of these *N*-arylisatins used methodology developed by Chan and Lam (**Scheme 14**).[58,59]

Scheme 14

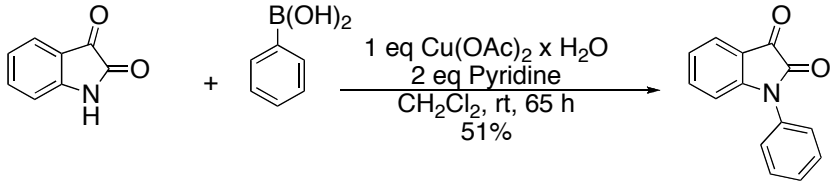

This Chan-Lam methodology was successful at converting isatin to *N*-phenylisatin in 51% yield over 65 hours. The time of the reaction was modified for the substituted isatin scaffolds as the reaction was completed in a 24-hour period (**Scheme 15**).

Scheme 15

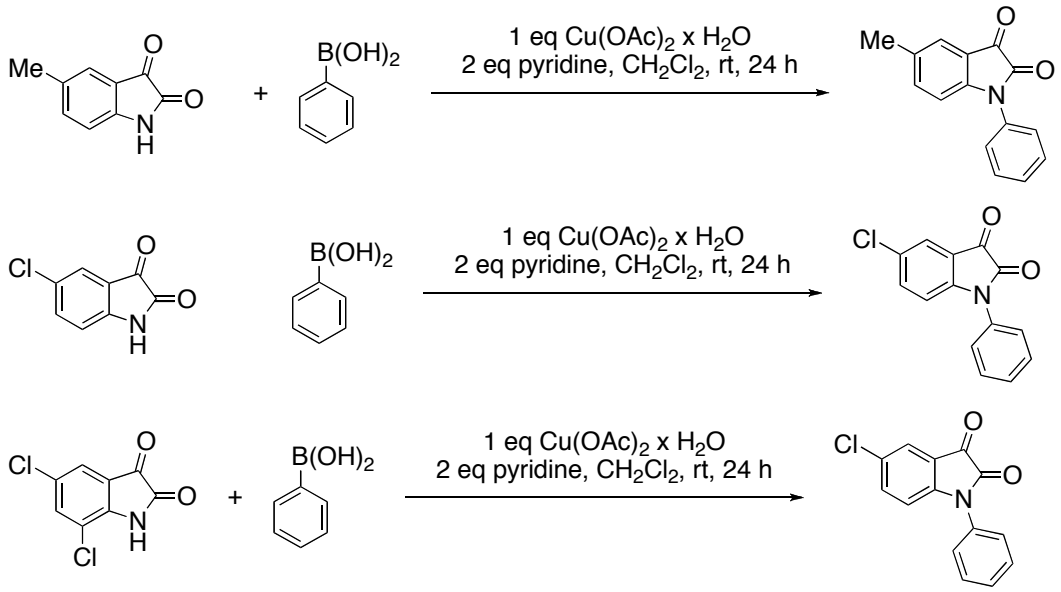

The appropriate isatin scaffold was dissolved in dichloromethane (DCM), resulting in a bright orange solution. Subsequent addition of the base pyridine and copper (II) acetate led to a dark purple solution. The dark purple color subsided upon addition of the desired boronic acid. The coupling was moderately successful for both the 5-methyl and 5-chloroisatin scaffolds (**Table 10**).

Table 10: Yields for 5-Methyl and 5-Chloro-*N*-Arylisatins

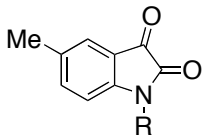	Yield	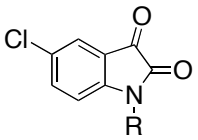	Yield
	16%		32%
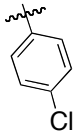	25%	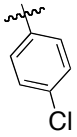	41%
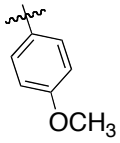	34%	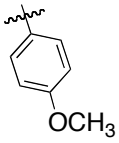	23%
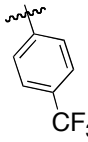	5%	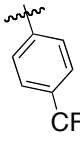	15%

The initial Chan-Lam test reaction failed to yield any of the 5,7-dichloro-*N*-phenylisatin derivatives with only starting material recovered. Therefore, a series of reaction conditions was screened to examine viable conditions for the coupling of the 5,7-dichloroisatin to phenyl boronic acid (**Table 11**).

Table 11: 5,7-Dichloroisatin Chan-Lam Reactions

	Substrate	Boronic Acid	$Cu(OAc)_2$	Base	Time	Yield
1	0.1 mmol	0.11 mmol	0.1 mmol	2 eq NEt_3	24 h	n.r.
2	0.1 mmol	0.11 mmol	0.2 mmol	2 eq NEt_3	24 h	n.r.
3	0.2 mmol	0.22 mmol	0.2 mmol	2 eq Pyridine	48 h	n.r.

Reaction Conditions: Addition of crushed 4 Å mol sieves to each reaction vessel

The exchange of pyridine for triethylamine, **1**, had no affect on reactivity. The same was true for increasing the amount of copper (II) acetate, reactions **2** and **3**; starting material was isolated in all cases.

The lack of activity in the Chan-Lam coupling led to the investigation of other *N*-arylation procedures by Buchwald and co-workers (**Scheme 16**).[60-62]

Scheme 16

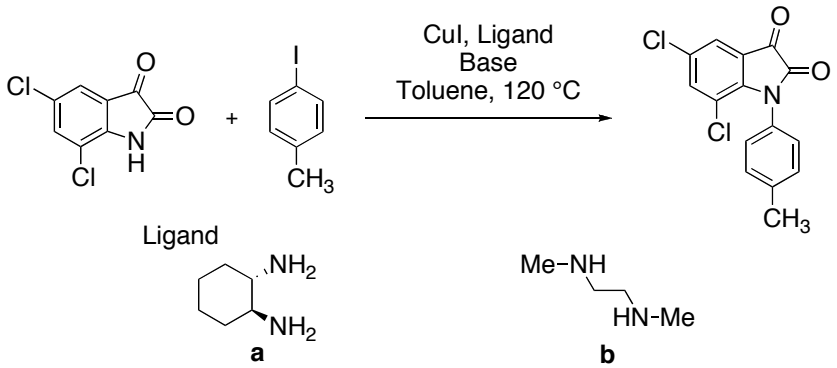

The Buchwald modification, of the Goldberg amidation reaction, uses inexpensive 1,2-diamine ligands to facilitate the copper-catalyzed aryl amidation reaction. The 1,2-diamine ligands we chose to study were racemic *trans*-1,2-cyclohexanediamine (**a, reactions 1-3**) and *N,N'*-dimethylethane-1,2-diamine (**b, reactions 4-6**),(**Table 12**).

Table 12: 5,7-Dichloroisatin Buchwald Reactions

	Ligand	Substrate	4-Iodotoluene	CuI	Base	Time	Yield
1	a	0.1 mmol	0.11 mmol	5 mol%	2 eq K_3PO_4	24 h	n.r.
2	a	0.1 mmol	0.11 mmol	5 mol%	2 eq K_2CO_3	24 h	n.r.
3	a	0.1 mmol	0.11 mmol	10 mol%	2 eq K_2CO_3	24 h	n.r.
4	b	0.1 mmol	0.11 mmol	5 mol%	2 eq K_3PO_4	24 h	n.r.
5	b	0.1 mmol	0.11 mmol	5 mol%	2 eq K_2CO_3	24 h	n.r.
6	b	0.1 mmol	0.11 mmol	10 mol%	2 eq K_2CO_3	24 h	n.r.

The results, shown in **Table 12**, confirm that 5,7-dichloroisatin is not a good candidate for *N*-arylation. All of the reactions yielded starting material upon quenching with acid. The steric hindrance and electron-withdrawing nature of the chloro groups may lead to the lack of reactivity. Another plausible explanation for the lack of reactivity is the formation of an insoluble complex between the deprotonated 5,7-dichloroisatin with the copper catalyst (**Scheme 17**).

Scheme 17

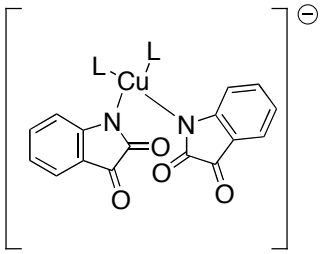

Additional attempts of *N*-arylation using palladium sources were also unsuccessful.[63] Therefore 5,7-dichloroisatin was not used as a scaffold for the SAR study. The 5-methyl and 5-chloroisatin derivatives were submitted for biological evaluation. None of the 5-methyl or 5-chloro-*N*-arylisatin derivatives demonstrated biological activity (**Tables 13** and **14**).

Table 13: Biological Evaluation of 5-Methyl-*N*-arylisatins

	Microtubule Assay[b]	MCF-7	NCI/ADR-RES[a]
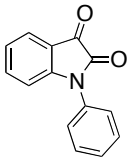	IC_{50} 3.2 μM $IC_{50}/IC_{50(col)}$: 0.64	IC_{50} >100 μM	IC_{50} >100 μM
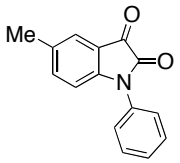	IC_{50} 6.4 μM $IC_{50}/IC_{50(col)}$: 1.3	IC_{50} >100 μM	IC_{50} >100 μM
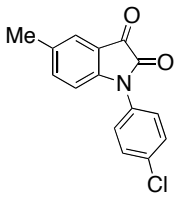	IC_{50} >25 μM $IC_{50}/IC_{50(col)}$: N/A	IC_{50} >100 μM	IC_{50} >100 μM
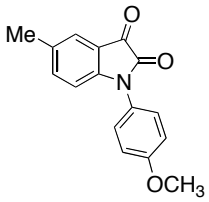	IC_{50} >25 μM $IC_{50}/IC_{50(col)}$: N/A	IC_{50} 18 μM	IC_{50} 7 μM
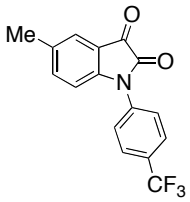	IC_{50} >100 μM $IC_{50}/IC_{50(col)}$: N/A	IC_{50} >100 μM	IC_{50} >100 μM

[a] NCI/ADR-RES formerly known as MCF7-ADR

[b] IC_{50} values for Colchicine is 5 μM

Table 14: Biological Evaluation of 5-Chloro-*N*-arylisatins

	Microtubule Assay[b]	MCF-7	NCI/ADR-RES[a]
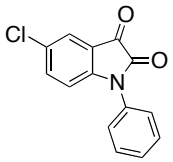	IC_{50} 20 μM $IC_{50}/IC_{50(col)}$: 4.0	IC_{50} >100 μM	IC_{50} >100 μM
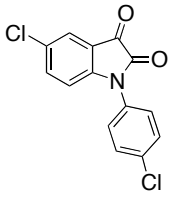	IC_{50} >100 μM $IC_{50}/IC_{50(col)}$: N/A	IC_{50} >100 μM	IC_{50} >100 μM
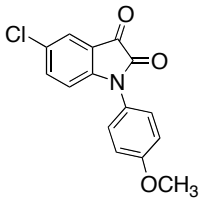	IC_{50} >100 μM $IC_{50}/IC_{50(col)}$: N/A	IC_{50} >100 μM	IC_{50} >100 μM
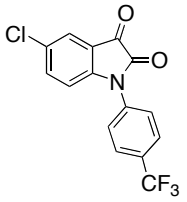	IC_{50} 22.2 μM $IC_{50}/IC_{50(col)}$: 4.4	IC_{50} >100 μM	IC_{50} >100 μM

[a] NCI/ADR-RES formerly known as MCF7-ADR
[b] IC_{50} values for Colchicine is 5 μM

Closing Remarks

The SAR study showed that substitutions in the 5- and 7- positions of the aromatic ring combined with *N*-substitutions increased the disruption of microtubule assembly. The 7-phenylisatin and *N*-arylisatin derivatives were inactive in all of the biological assays. Several of the 5-chloro-*N*-alkylisatins and the 5,7-dichloro-*N*-alkylisatins were cytotoxic in both MCF-7 and NCI/ADR-RES cell lines. 5,7-Dichloro-*N*-(1-propyl)isatin exhibited an IC_{50} value of 3.0 μM in the microtubule assembly assay and was selectively cytotoxic in the NCI/ADR-RES cell line, IC_{50} = 2.7 μM. Similarly, 5,7-dichloro-*N*-(ethyl)isatin and 5,7-dichloro-*N*-(1-butyl)isatin inhibited microtubule assembly with IC_{50} values of 3.2 μM and 3.5 μM, respectively, and IC_{50} values of 7.0 μM (1-ethyl) and 1.1 μM (1-butyl) in NCI/ADR-RES cells. 5,7-Dichloro-*N*-(4-bromobenzyl)isatin was the most active compound against MCF-7 cells, IC_{50} = 2.1 μM. This compound was also active against the drug resistant line, IC_{50} = 2.2 μM. To date the most cytotoxic compound tested is 5-methyl-*N*-(1-propyl)isatin, with an IC_{50} value of 52 nM (microtubule assembly IC_{50} = 2.6 μM) in the drug resistant cancer cell line NCI/ADR-RES.

Experimental Section

Materials and Methods. ^{1}H and ^{13}C nuclear magnetic resonance spectra were recorded using a Bruker DRX 400 MHz spectrophotometer. All chemical shifts were recorded as parts per million (ppm), and all samples were dissolved in $CDCl_3$ using tetramethylsilane (TMS) as the internal standard. Mass spectra were obtained from a ESI-TOF HS mass spectrometer (Bruker, BioTOF II, Bruker BioSpin Corp., Billerica, MA, USA). Melting points were collected using a Fisher-Johns melting point apparatus and are uncorrected.

All moisture-sensitive reactions were performed using either oven or flame dried glassware under positive pressure of nitrogen unless otherwise noted. Solvents and reagents that are commercially available were used without further purification unless otherwise noted. All silica gel (230-400 mesh) used for column chromatography was purchased from VWR Scientific Products. All compounds were concentrated using standard rotovap and high-vacuum techniques where concentration was noted. Flash chromatography was performed using 60 Å porosity silica gel from Sorbent Technologies under a positive pressure of nitrogen.

Microtubule Assembly Assay. The reactions were performed in 96-well plates in a volume of 120 μL per well. The wells contained PEM buffer (0.1 M Pipes, 1 mM $MgSO_4$, 1 mM EGTA, pH 6.9), 4% DMSO, 10 μM DAPI, 2

mg/mL microtubule protein and varying concentrations of the compound. The plates were incubated at 37 ºC for 30 min after which the fluorescence was measured in a multi-plate reader. The readings were corrected for a control lacking the compound.

Cytotoxicity Assay. The cytotoxic effects of test compounds were measured using a modification of the procedure developed by the National Cancer Institute (NCI). Originally the assay was performed using sulforhodamine to measure protein content,[64] but they later modified it to use a colorimetric redox dye, 2-(4,5-dimethylthiazol-2-yl)-2,5-diphenyltetrazolium (MTT).[65] We have again modified the procedure to use an alternative, water soluble redox dye, resofurin (Alamar Blue™). The dye also has the advantage that the red-shifted fluorescence of the dye reduces interference from auto-fluorescent compounds. A direct comparison measuring cytotoxicity of standard compounds with a number of cell lines using this dye compared to the original sulforhodamine assay in our laboratories produced identical results (unpublished data).

Two cell lines from NCI were used in this study (MCF-7 and MCF-7/ADR). The former cell line is a human breast adenocarcinoma cell line, and the later a derivative that is multi-drug resistant due to over expression of p-glycoprotein.

Stock cultures were grown in T-75 flasks containing 40 mL of RPMI-1640 medium with glutamine, bicarbonate and 10% fetal bovine serum. After growth for 48 hours, cells (in exponential-phase culture) were dissociated with 0.25% trypsin in buffer (contaiing 0.38 g/L of EDTA·4Na^+ in Hanks' Balanced Salt Solution: without $CaCl_2$, $MgCl_2 \cdot 6H_2O$, and $MgSO_4 \cdot 7H_2O$, with phenol red) and harvested by centrifugation at 125 g for 5 min. The supernatant containing trypsin was removed and the cells re-suspended in new culture medium, the cell density was adjusted to$1x10^5$ cells/mL.

Cells were dispensed as 50 μL aliquots into 96-well microtiter plates (density of 5,000 cells/well) and incubated for 24 hours at 37 ^oC and 5.0% CO_2 in a humidified tissue culture incubator. During this time the cells attached to the bottoms of the microplate wells. At this point, 50 μL of culture medium containing test compounds at various concentrations were added to the wells and the plates incubated for 48 hours at 37 ^oC and 5.0% CO_2 in a humidified tissue culture incubator. The plates were then removed and 25 μL of a stock solution of Alamar Blue™(Invitrogen) was added and the plates re-incubated for 2 hours.. The stock solution was prepared bv making a 1:10 dilution of the supplied reagent in media.

After incubation the plates were remove and the fluorescence of the dye was measured spectrofluorimetrically using an excitation wavelength of 560 nm and an emission wavelength of 590 nm using either a Molecular

Devices Spectromax 2e™ multimode plate reader or a LJL Analyst AD™ multimode plate reader.

Taxol (Invitrogen) and Colchicine (Sigma) were used as standards, and prepared in 100% DMSO. The initial highest final concentrations of Taxol and Colchicine in the test were 2500 ng/mL (2930 nM) and 60 μM respectively at 1% DMSO in RPMI culture medium. Four fold serial dilutions were made using RPMI culture medium containing 1% DMSO, and then 50 μL of these solutions added to the cells as described above. Tests were conducted with 3 replicates of the dose-response curve, and results were average before being analyzed. IC_{50} curves and results were calculated using GraphPad (Prism software).

General Procedure A: Suzuki cross-couplings of 7-bromoisatin. A solution of 7-bromoisatin (0.10 mmol, 1 eq), in THF/H_2O (v:v, 4 mL) under a N_2 atmosphere was stirred. Solid K_2CO_3 (0.2 mmol, 2 eq) and $Pd(PPh_3)_4$ (2 mol %) were added. The reaction was stirred at rt for 1 h. The appropriate aryl trifluoroborate (0.11 mmol, 1.1 eq) was added and the reaction was stirred at 60 °C for 12 h, until the starting material had been consumed (TLC). The reaction mixture was then transferred to a separatory funnel containing 10% aq. HCl (10 mL) and DCM (10 mL). The layers were separated and the aqueous layer was extracted twice more with DCM (5 mL). The combined organic layers were then washed with saturated aq. NaCl (20 mL) and dried

with $MgSO_4$, concentrated and purified by flash chromatography on silica gel using isocratic elution with ethyl acetate.

General Procedure B: *N*-Alkylation of isatin scaffolds. A solution of the appropriate indoline-2,3-dione (0.20 mmol, 1 eq), in anhydrous DMF (2 mL) cooled to 0 °C under a N_2 atmosphere was stirred. Solid Cs_2CO_3 (0.22 mmol, 1.1 eq) was added in one portion. The reaction was brought to rt and stirred for 1 h. The appropriate alkylating agent (0.20 mmol, 1 eq) was added and the reaction was stirred at 50 °C for 12 h, until the starting material had been consumed (TLC). The reaction mixture was then transferred to a separatory funnel containing 10% aq. HCl (10 mL), distilled H_2O (10 mL) and diethyl ether (10 mL). The layers were separated and the aqueous layer was extracted twice more with diethyl ether (5 mL). The combined organic layers were then washed with saturated aq. NaCl (20 mL) and dried with $MgSO_4$, concentrated and purified by flash chromatography on silica gel using isocratic elution with ethyl acetate.

General Procedure C: Chan-Lam methodology for *N*-arylation of isatin scaffolds. A slurry of the appropriate indoline-2,3-dione (0.25 mmol, 1 eq) in anhydrous DCM (1 mL) was prepared. Solid $Cu(OAc)_2 \times H_2O$ (0.25 mmol, 1 eq), the appropriate arylboronic acid (0.50 mmol, 2 eq), and pyrdine (0.50 mmol, 2 eq) were added. The reaction was stirred at rt for 24 h, until the starting material had been consumed (TLC). The reaction mixture was then

transferred to a separatory funnel containing 10% aq. HCl (10 mL) and DCM (10 mL). The layers were separated and the aqueous layer was extracted twice more with DCM (5 mL). The combined organic layers were then washed with saturated aq. NaCl (20 mL) and dried with $MgSO_4$, concentrated and purified by flash chromatography on silica gel using isocratic elution with ethyl acetate.

General Procedure C: Buchwald methodology for *N*-arylation of isatin scaffolds. A two-neck round-bottom was charged with 5,7-dichloroisatin (0.14 mmol, 1.2 eq), anhydrous toluene (5 mL), CuI (5 mol %), appropriate ligand (10 mol %), and the 4-methyl-iodobenzene (0.1 mmol, 1 eq). The reaction was stirred at rt for 15 min. A solution of the appropriate base (1.0 M in H_2O, 0.2 mmol, 2 eq) was added dropwise to the reaction. A reflux condenser was fitted to the round-bottom and the reaction was heated to 120 °C for 24 h.

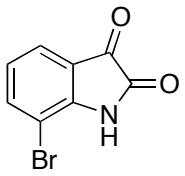

7-Bromoisatin. A round-bottom flask was charged with chloral hydrate (0.55 g, 3.3 mmol), anhydrous Na_2SO_4 (3.41 g, 24.0 mmol), and EtOH/H_2O (v:v, 4 mL). The solution was acidified to a pH 1 with 6 N HCl. The reaction was stirred at 40 °C until the solution became clear. Solid 2-bromoaniline (0.50 g, 3.0 mmol) and $NH_2OH{\cdot}HCl$ (0.70 g, 10 mmol) were added and the reaction was heated to 100 °C for 40 min. The reaction was cooled to rt and the isonitrosoacetanilide precipitate was formed. The precipitate was collected via filtration and dried under vacuum for 4 h. The dried precipitate was then dissolved in concentrated H_2SO_4 (10 mL) and heated to 60 °C for 1 h. The reaction was cooled to rt and poured over cracked ice (20 mL) yielding an orange precipitate. The precipitate was collected via filtration and dried under vacuum overnight to give 0.56 g of the title compound as an orange solid (85%), mp 144-146 ºC. ^{1}H NMR (400 MHz, $CDCl_3$) δ 7.27 (1H, t, J = 7.5 Hz), 7.95 (1H, d, J = 7.5,1.5 Hz), 8.0 (1H, s, br), 8.06 (1H, d, J = 7.5, 1.5 Hz). ^{13}C NMR (100 MHz, $CDCl_3$) δ 119, 123, 125, 126, 137.6, 143.3, 160.2, 184.7. HRMS calcd for $C_8H_4BrNO_2$, 224.9425; found 225.0326.

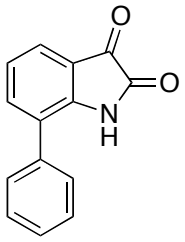

7-Phenylisatin was prepared using general procedure A, (60%), orange solid, mp 249-250 ºC. ^{1}H NMR (400 MHz, $CDCl_3$) δ to give 0.014 g of the title compound as an orange solid (60%), (100 MHz, $CDCl_3$) δ 7.08 (2H, m, *J* = 7.5, 7.5, 1.5, 1.5 Hz), 7.41 (1H, t, *J* = 7.5, 7.5, 1.5, 1.5 Hz), 7.44 (1H, d, *J* = 7.5, 7.5 Hz), 7.51 (2H, m, *J* = 7.5, 7.5, 1.5, 1.5 Hz), 7.97 (1H, dd, *J* = 7.5, 1.5 Hz), 8.05 (1H, dd, *J* = 7.5, 1.5 Hz), 8.0 (1H, s, br), ^{13}C NMR (400 MHz, $CDCl_3$) δ 118.2, 122, 124.6, 124.7, 127.6, 127.9, 127.9, 129.2, 129.2, 130.1, 138.3, 139.8, 159.3, 184.3. HRMS: calcd for $C_{14}H_9NO_2$, 223.0633; found, 222.9989.

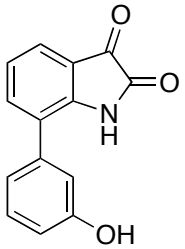

7-(3-Hydroxyphenyl)isatin was prepared using general procedure A, (74%), orange solid, mp 360-362 ºC. ^{1}H NMR (400 MHz, $CDCl_3$) δ 5.35 (1H, s, br), 6.91 (1H, dd, *J* = 7.5, 1.5, 1.5 Hz), 7.08 (1H, dd, *J* = 7.5, 1.5, 1.5 Hz), 7.32 (1H, dd, *J* = 1.5, 1.5 Hz), 7.34 (1H, t, *J* = 7.5, 7.5 Hz), 7.44 (1H, t, *J* = 7.5, 7.5 Hz), 8.0 (1H, s, br), 8.05 (1H, d, *J* = 1.5, 7.5 Hz). ^{13}C NMR (100 MHz, $CDCl_3$) δ 114.8, 115.9, 118.2, 121, 122.6, 124.6, 124.8, 127.9, 127.9, 129.8, 130.2,

137.9, 138.3, 157.6, 159.3, 184.3. HRMS: calcd for $C_{14}H_9NO_3$, 229.0582; found, 230.0019.

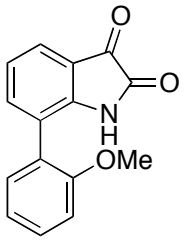

7-(2-Methoxyphenyl)isatin was prepared using general procedure A, (32%), orange solid, mp 295-297 ºC. ^{1}H NMR (400 MHz, $CDCl_3$) δ 3.83 (3H, s), 7.05 (1H, d, *J* = 7.5, 1.5 Hz), 7.08 (1H, t, *J* = 7.5, 7.5 Hz), 7.32 (1H, t, *J* = 7.5, 7.5, 1.5 Hz), 7.44 (1H, t, *J* = 7.5, 7.5 Hz), 7.68 (1H, d, *J* = 7.5, 1.5 Hz), 8.0 (1H, s, br), 8.05 (1H, d, *J* = 7.5, 1.5 Hz). ^{13}C NMR (100 MHz, $CDCl_3$) δ 56.2, 116.8, 118.2, 121.6, 122.3, 124.6, 124.8, 125.7, 127.9, 129.9, 130.8, 137.9, 157.7, 159.3, 184.3. HRMS: calcd for $C_{15}H_{11}NO_3$, 253.0739; found, 253.0978.

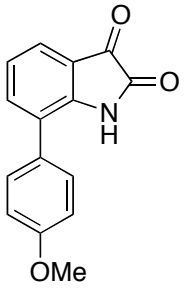

7-(4-Methoxyphenyl)isatin was prepared using general procedure A, (74%), orange solid, mp 295-297 ºC. ^{1}H NMR (400 MHz, $CDCl_3$) δ 3.83 (3H, s), 7.05 (2H, d, *J* = 7.5, 1.5 Hz), 7.44 (1H, t, *J* = 7.5, 7.5 Hz), 7.68 (2H, d, *J* = 7.5, 1.5 Hz), 7.97 (1H, d, *J* = 7.5, 1.5 Hz), 8.0 (1H, s, br), 8.05 (1H, d, *J* = 7.5, 1.5 Hz). ^{13}C NMR (100 MHz, $CDCl_3$) δ 55.2, 114.8, 114.8, 118.2, 122.3, 124.6, 124.8,

129.9, 130.1, 130.1, 132.2, 137.9, 159.3, 159.5, 184.3. HRMS: calcd for $C_{15}H_{11}NO_3$, 253.0739; found, 253.0978.

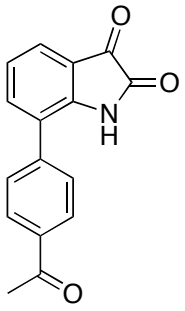

7-(4-Acetylphenyl)isatin was prepared using general procedure A, (44%), orange solid, mp 334-337 °C. ^{1}H NMR (400 MHz, $CDCl_3$) δ 2.50 (3H, s), 8.00 (2H, d, *J* = 7.5, 1.5 Hz), 7.75 (2H, d, *J* = 7.3, 1.5 Hz), 8.05 (1H, d, *J* = 7.5, 1.5 Hz), 7.44 (1H, t, *J* = 7.6, 1.8 Hz), 7.97 (1H, d, *J* = 7.5, 1.5 Hz), 8.0 (1H, s, br). ^{13}C NMR (100 MHz, $CDCl_3$) δ 26.6, 197.0, 129.3, 127.8, 122.3, 130.0, 129.3, 127.8, 135.6, 144.1, 124.6, 124.7, 118.2, 138.3, 184.3, 159.3. HRMS: calcd for $C_{16}H_{11}NO_3$, 265.0739; found, 265.0834.

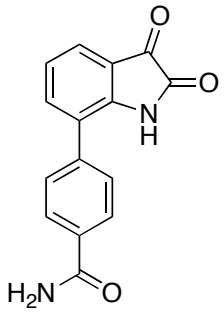

7-(4-Amidophenyl)isatin was prepared using general procedure A, (19%), orange solid, mp 404-407 °C. ^{1}H NMR (400 MHz, $CDCl_3$) δ 7.5 (2H, s, br), 8.09 (2H, d, *J* = 7.5, 1.5 Hz), 7.82 (2H, d, *J* = 7.5, 1.5 Hz), 8.05 (1H, d, *J* = 7.5, 1.5 Hz), 7.44 (1H, t, *J* = 7.5 Hz), 7.97 (1H, d, *J* = 7.5, 1.5 Hz), 8.0 (1H, s,

br). ^{13}C NMR (100 MHz, $CDCl_3$) δ 168.0, 130.2, 128.0, 122.3, 130.0, 130.2, 128.0, 133.1, 143.1, 124.6, 124.7, 118.2, 138.3, 184.4, 159.3. HRMS: calcd for $C_{15}H_{10}N_2O_3$, 266.0691; found, 265.0714.

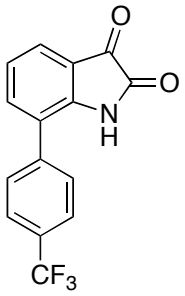

7-(4-(Trifluoro-methyl)phenyl)isatin was prepared using general procedure A, (9%), orange solid, mp 278-280 °C. ^1H NMR (400 MHz, $CDCl_3$) δ 7.68 (2H, d, *J* = 7.5, 1.5 Hz), 7.38 (2H, d, *J* = 7.5, 1.6 Hz), 8.05 (1H, d, *J* = 7.5, 1.5 Hz), 7.44 (1H, t, *J* = 7.5, 1.3 Hz), 7.97 (1H, d, *J* = 7.7, 1.5 Hz), 8.0 (1H, s, br). ^{13}C NMR (100 MHz, $CDCl_3$) δ 124.1, 125.6, 128.2, 122.3,130.0, 125.6, 128.2, 129.9, 143.0, 124.6, 124.7, 118.2, 138.3, 184.3, 159.3. HRMS: calcd for $C_{15}H_8F_3NO_2$, 291.0507; found, 291.1067.

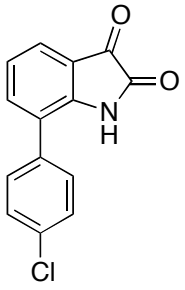

7-(4-Chlorophenyl)isatin was prepared using general procedure A, (24%), orange solid, mp 292-294 °C. ^1H NMR (400 MHz, $CDCl_3$) δ 7.73 (2H, d, *J* = 7.4, 1.5 Hz), 7.55 (2H, d, *J* = 7.5, 1.5 Hz), 8.05 (1H, d, *J* = 7.7, 1.4 Hz), 7.44

(1H, t, *J* = 7.5, 1.5 Hz), 7.97 (1H, d, *J* = 7.5, 1.5 Hz), 8.0 (1H, s, br). ^{13}C NMR (100 MHz, $CDCl_3$) δ129.3, 122.3, 130.0, 129.3, 129.3, 129.3, 137.8, 124.6, 124.7, 133.2, 118.2, 138.3, 184.3, 159.3. HRMS: calcd for $C_{14}H_8ClNO_2$, 257.0244; found, 257.0364.

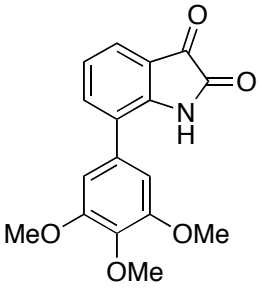

7-(3,4,5-Trimethoxyphenyl)isatin was prepared using general procedure A, (46%), orange solid, mp 389-391 °C. ^{1}H NMR (400 MHz, $CDCl_3$) δ 8.0 (1H, s, br), 8.05 (1H, d, *J* = 7.6, 1.5 Hz), 7.98 (1H, d, *J* = 7.4, 1.6 Hz), 7.45 (1H, t, *J* = 7.5, 7.5 Hz), 6.51 (2H, dd, *J* = 1.5, 1.5 Hz), 3.83 (9H, s). ^{13}C NMR (100 MHz, $CDCl_3$) δ 56.1, 56.1, 61, 106.3, 106.3, 118.3, 122.3, 124.5, 124.6, 130.0, 131.4, 138.3, 138.1, 153.1, 153.1, 159.3, 184.3. HRMS: calcd for $C_{17}H_{15}NO_5$, 313.3047; found, 313.0950.

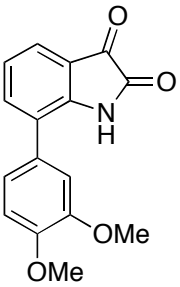

7-(3,4-Dimethoxyphenyl)isatin was prepared using general procedure A, (24%), orange solid, mp 341-343 °C. ^{1}H NMR (400 MHz, $CDCl_3$) δ 8.0 (1H, s,

br), 8.05 (1H, d, *J* = 7.4, 1.5 Hz), 7.98 (1H, d, *J* = 7.4, 1.6 Hz), 7.45 (1H, t, *J* = 7.5, 7.5 Hz), 7.24 (1H, d, *J* = 7.4, 1.5 Hz), 6.94 (1H, d, *J* = 7.5 Hz), 6.95 (1H, d, *J* = 7.5 Hz), 3.83 (6H, s). ^{13}C NMR (100 MHz, $CDCl_3$) δ 56.1, 56.1, 61, 111.0, 114.0, 118.2, 122.2, 122.4, 124.6, 124.7, 129.8, 130.0, 138.3, 148.7, 150.3, 159.3, 184.3. HRMS: calcd for $C_{16}H_{13}NO_4$, 283.2787; found, 283.0845.

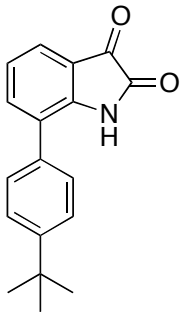

7-(4-t-Butylphenyl)isatin was prepared using general procedure A, (10%), orange solid, mp 310-312 °C. ^{1}H NMR (400 MHz, $CDCl_3$) δ 8.0 (1H, s, br), 8.05 (1H, d, *J* = 7.4, 1.5 Hz), 7.97 (1H, d, *J* = 7.8, 1.7 Hz), 7.44 (1H, t, *J* = 7.6, 7.6 Hz), 7.37 (2H, dd, *J* = 7.5, 7.5, 1.5, 1.5 Hz), 7.38 (2H, dd, *J* = 7.5, 7.5, 1.5, 1.5 Hz), 1.35 (9H, s). ^{13}C NMR (100 MHz, $CDCl_3$) δ 31.3, 31.3, 31.3, 34.2, 118.2, 122.4, 124.6, 124.7, 125.5, 125.5, 127.5, 127.5, 130.0, 136.6, 138.3, 150.2, 159.3, 184.3. HRMS: calcd for $C_{18}H_{17}NO_2$, 279.3331; found, 279.1259.

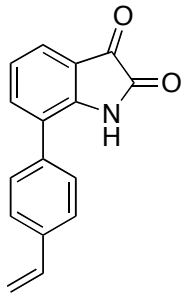

7-Vinylisatin was prepared using general procedure A, (65%), orange solid, mp 284-286 ºC. ^{1}H NMR (400 MHz, $CDCl_3$) δ 8.0 (1H, s, br), 7.89 (1H, d, *J* = 7.4, 1.4 Hz), 7.64 (1H, d, *J* = 7.6, 1.3 Hz), 7.22 (1H, t, *J* = 7.6, 7.6) 6.90 (1H, dd, *J* = 16.8, 10.0 Hz), 5.44 (1H, d, *J* = 2.1, 16.8 Hz), 5.34 (1H, d, *J* = 2.1, 10.0 Hz). ^{13}C NMR (100 MHz, $CDCl_3$) δ114.3, 117.8, 124.8, 124.9, 130.7, 134.5, 134.6, 137.2, 159.3, 184.3. HRMS: calcd for $C_{14}H_8ClNO_2$, 173.1681; found, 173.0477.

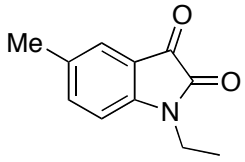

***N*-(Ethyl)-5-methylisatin** was prepared using general procedure B, (83%), orange solid, mp 185-187 °C. ^{1}H NMR (400 MHz, $CDCl_3$) δ 1.32 (3H, t, *J* = 8.0 Hz), 2.35 (3H, s), 4.28 (2H, q, *J* = 8.0 Hz), 7.50 (1H, dd, *J* = 7.5, 1.5 Hz), 7.58 (1H, s, *J* = 1.5 Hz), 7.88 (1H, d, *J* = 7.5 Hz). ^{13}C NMR (100 MHz, $CDCl_3$) δ 13.8, 21.3, 42.7, 124.1, 137.5, 116.5, 117.8, 145.1, 180.0, 160.0. HRMS: calcd for $C_{11}H_{11}NO_2$, 189.0790; found, 189.1125.

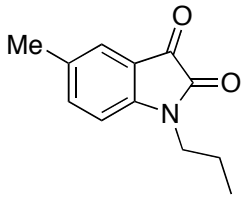

***N*-(1-Propyl)-5-methylisatin** was prepared using general procedure B, (48%), orange solid, mp 195-197 °C. ^{1}H NMR (400 MHz, $CDCl_3$) δ 0.90 (3H, t, *J* = 8.0 Hz), 1.73 (2H, m, *J* = 7.1, 8.0 Hz), 2.34 (3H, s), 4.28 (2H, t, *J* = 7.1 Hz), 7.50 (1H, d, *J* = 7.5, 1.5 Hz), 7.58 (1H, s), 7.88 (1H, d, *J* = 7.5, 1.5 Hz). ^{13}C NMR (100 MHz, $CDCl_3$) δ 11.5, 20.3, 21.3, 45.1, 116.5, 117.6, 124.0, 124.1, 137.5, 145.2, 160.1, 179.9. HRMS: calcd for $C_{12}H_{13}NO_2$, 203.2371; found, 203.0946.

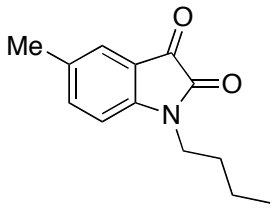

***N*-(1-Butyl)-5-methylisatin** was prepared using general procedure B, (58%), orange solid, mp 207-208 °C. ^{1}H NMR (400 MHz, $CDCl_3$) δ 0.90 (3H, t, *J* = 8.0 Hz), 1.31 (2H, m, *J* = 7.1, 8.0 Hz), 1.52 (2H, m, *J* = 7.1, 7.1 Hz), 2.34 (3H, s), 3.97 (2H, t, *J* = 7.1 Hz), 7.50 (1H, dd, *J* = 7.5, 1.5 Hz), 7.58 (1H, s), 7.88 (1H, d, *J* = 7.5 Hz). ^{13}C NMR (100 MHz, $CDCl_3$) δ 13.8, 20.1, 21.3, 29.6, 42.7, 124.1, 137.5, 124.0, 116.5, 117.8, 145.1, 180.0, 160.0. HRMS: calcd for $C_{13}H_{15}NO_2$, 217.2637; found, 217.1103.

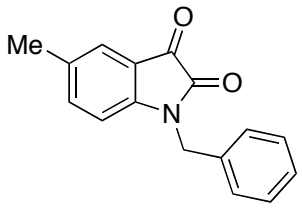

***N*-(Benzyl)-5-methylisatin** was prepared using general procedure B, (52%), orange solid, mp 268-270 °C. ^{1}H NMR (400 MHz, $CDCl_3$) δ 2.34 (3H, s), 4.94 (2H, s), 7.26 (1H, m, *J* = 7.5, 7.5, 1.5, 1.5 Hz), 7.33 (2H, m, 7.5, 7.5, 1.5 Hz), 7.49 (1H, d, *J* = 7.5, 1.5 Hz), 7.58 (1H, s), 7.88 (1H, dd, 7.5, 1.5). ^{13}C NMR (100 MHz, $CDCl_3$) δ 21.3, 47.6, 116.5, 117.6, 124.0, 124.1, 126.7, 126.9, 126.9, 128.5, 128.5, 136.1, 137.4, 145.1, 160.4, 179.9. HRMS: calcd for $C_{16}H_{13}NO_2$, 251.2799; found, 251.0946.

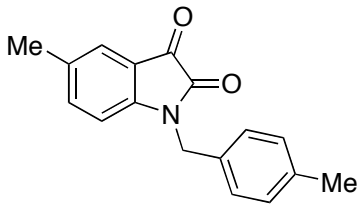

***N*-(4-Methylbenzyl)-5-methylisatin** was prepared using general procedure B, (68%), orange solid, mp 290-293 °C. ^{1}H NMR (400 MHz, $CDCl_3$) δ 2.34 (6H, s), 4.94 (2H, s), 7.11 (4H, dd, *J* = 7.5, 7.5, 1.5, 1.5 Hz), 7.49 (1H, d, *J* = 7.5, 1.5 Hz), 7.58 (1H, s), 7.88 (1H, dd, 7.5, 1.5). ^{13}C NMR (100 MHz, $CDCl_3$) δ 21.3, 21.3, 47.6, 116.5, 117.6, 124.0, 124.1, 128.1, 128.8, 128.8, 133.1, 136.1, 137.4, 145.1, 160.4, 179.9. HRMS: calcd for $C_{17}H_{15}NO_2$, 265.3065; found, 265.1103.

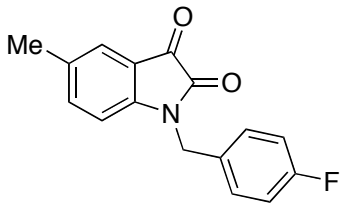

***N*-(4-Fluorobenzyl)-5-methylisatin** was prepared using general procedure B, (86%), orange solid, mp 281-282 °C. ^{1}H NMR (400 MHz, $CDCl_3$) δ 2.34 (3H, s), 4.94 (2H, s), 7.12 (2H, dd, *J* = 8.0, 7.5, 1.5 Hz), 7.39 (2H, dd, *J* = 7.5, 1.5, 5.0 Hz), 7.49 (1H, d, *J* = 7.5, 1.5 Hz), 7.58 (1H, s), 7.88 (1H, dd, 7.5, 1.5). ^{13}C NMR (100 MHz, $CDCl_3$) δ 21.3, 47.6, 115.3, 115.3, 116.5, 117.6, 124.0, 124.1, 128.5, 128.5, 131.7, 137.4, 145.1, 160.4, 160.9, 179.9. HRMS: calcd for $C_{16}H_{12}FNO_2$, 269.2704; found, 269.0852.

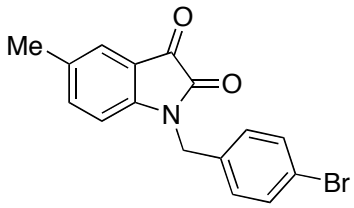

***N*-(4-Bromobenzyl)-5-methylisatin** was prepared using general procedure B, (96%), orange solid, mp 339-340 °C. ^{1}H NMR (400 MHz, $CDCl_3$) δ 2.34 (3H, s), 4.94 (2H, s), 7.12 (2H, dd, *J* = 7.5, 1.5 Hz), 7.39 (2H, dd, *J* = 7.5, 1.5, 5.0 Hz), 7.49 (1H, d, *J* = 7.5, 1.5 Hz), 7.58 (1H, s), 7.88 (1H, s). ^{13}C NMR (100 MHz, $CDCl_3$) δ 21.3, 47.6, 116.5, 117.6, 121.1, 124.0, 124.1, 129.1, 129.1, 131.4, 131.4, 135.1, 137.4, 145.1, 160.4, 179.9. HRMS: calcd for $C_{16}H_{12}BrNO_2$, 330.1760; found, 329.0051.

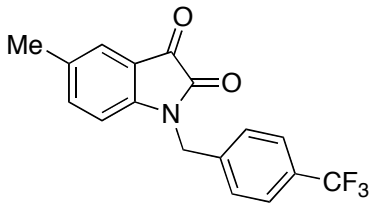

***N*-(4-(Trifluoro)methylbenzyl)-5-methylisatin** was prepared using general procedure B, (83%), orange solid, mp 295-297 °C. ^{1}H NMR (400 MHz, $CDCl_3$) δ 2.34 (3H, s), 4.94 (2H, s), 7.16 (2H, dd, *J* = 7.5, 1.5 Hz), 7.50 (2H, dd, *J* = 7.5, 1.5 Hz), 7.49 (1H, d, *J* = 7.5, 1.5 Hz), 7.58 (1H, s), 7.88 (1H, s). ^{13}C NMR (100 MHz, $CDCl_3$) δ 21.3, 47.6, 116.5, 117.6, 124.0, 124.1, 124.1, 124.9, 124.9, 128.5, 128.5, 129.1, 137.4, 139.4, 145.1, 160.4, 179.9. HRMS: calcd for $C_{17}H_{12}F_3NO_2$, 319.2779; found, 319.0820.

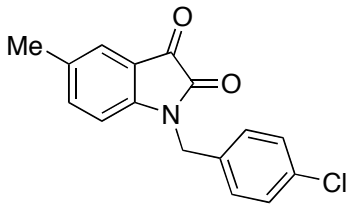

***N*-(4-Chlorobenzyl)-5-methylisatin** was prepared using general procedure B, (40%), orange solid, mp 309-310 °C. ^{1}H NMR (400 MHz, $CDCl_3$) δ 2.34 (3H, s), 4.94 (2H, s), 7.32 (2H, dd, *J* = 7.5, 1.5 Hz), 7.37 (2H, dd, *J* = 7.5, 1.5, 5.0 Hz), 7.49 (1H, d, *J* = 7.5, 1.5 Hz), 7.58 (1H, s), 7.88 (1H, s). ^{13}C NMR (100 MHz, $CDCl_3$) δ 21.3, 47.6, 116.5, 117.6, 124.0, 124.1, 128.6, 128.6, 129.3, 129.3, 132.3, 134.4, 137.4, 145.1, 160.4, 179.9. HRMS: calcd for $C_{16}H_{12}ClNO_2$, 285.0557; found, 285.7250.

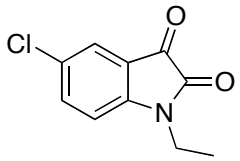

***N*-(Ethyl)-5-chloroisatin** was prepared using general procedure B, (65%), orange solid, mp 202-204 °C. ^{1}H NMR (400 MHz, $CDCl_3$) δ 1.32 (3H, t, *J* = 8.0 Hz), 4.28 (2H, q, *J* = 8.0 Hz), 7.75 (1H, dd, *J* = 7.5, 1.5 Hz), 7.79 (1H, s, *J* = 1.5 Hz), 7.94 (1H, d, *J* = 7.5 Hz). ^{13}C NMR (100 MHz, $CDCl_3$) δ 13.8, 42.7, 119.1, 124.7, 126.9, 134.8, 138.2, 146.2, 160.1, 179.9. HRMS: calcd for $C_{10}H_8ClNO_2$, 209.6290 found, 209.0244.

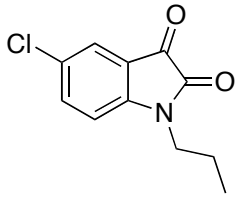

***N*-(1-Propyl)-5-chloroisatin** was prepared using general procedure B, (36%), orange solid, mp 215-216 °C. ^{1}H NMR (400 MHz, $CDCl_3$) δ 0.90 (3H, t, *J* = 8.0 Hz), 1.73 (2H, m, *J* = 7.1, 8.0 Hz), 4.28 (2H, t, *J* = 7.1 Hz), 7.75 (1H, dd, *J* = 7.5, 1.5 Hz), 7.79 (1H, s, *J* = 1.5 Hz), 7.94 (1H, d, *J* = 7.5 Hz). ^{13}C NMR (100 MHz, $CDCl_3$) δ 11.5, 20.3, 44.9, 119.6, 124.7, 126.9, 134.8, 138.2, 145.2, 160.1, 179.9. HRMS: calcd for $C_{11}H_{10}ClNO_2$, 223.6556; found, 223.0400.

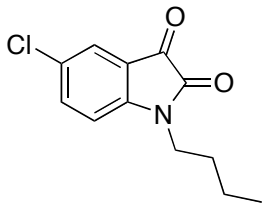

***N*-(1-Butyl)-5-chloroisatin** was prepared using general procedure B, (62%), orange solid, mp 225-227 °C. ^{1}H NMR (400 MHz, $CDCl_3$) δ 0.90 (3H, t, *J* = 8.0 Hz), 1.31 (2H, m, *J* = 7.1, 8.0 Hz), 1.52 (2H, m, *J* = 7.1, 7.1 Hz), 3.97 (2H, t, *J* = 7.1 Hz), 7.75 (1H, dd, *J* = 7.5, 1.5 Hz), 7.79 (1H, s, *J* = 1.5 Hz), 7.94 (1H, d, *J* = 7.5 Hz). ^{13}C NMR (100 MHz, $CDCl_3$) δ 13.8, 20.3, 29.6, 42.9, 119.6, 124.7, 126.9, 134.8, 138.2, 145.2, 160.1, 179.9.HRMS: calcd for $C_{12}H_{12}ClNO_2$, 237.6822; found, 237.0557.

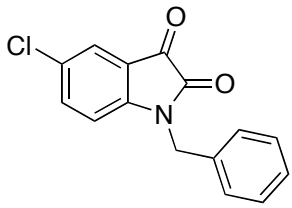

***N*-(Benzyl)-5-chloroisatin** was prepared using general procedure B, (84%), orange solid, mp 286-288 °C.^{1}H NMR (400 MHz, $CDCl_3$) δ 4.94 (2H, s), 7.23 (2H, m, *J* = 1.5, 7.5, 7.5 Hz), 7.26 (1H, m, *J* = 7.5, 7.5, 1.5, 1.5 Hz), 7.33 (2H, m, 7.5, 7.5, 1.5 Hz), 7.75 (1H, dd, *J* = 7.5, 1.5 Hz), 7.79 (1H, s, *J* = 1.5 Hz), 7.94 (1H, d, *J* = 7.5 Hz). ^{13}C NMR (100 MHz, $CDCl_3$) δ 47.6, 119.1, 124.7, 126.7, 126.9, 126.9, 126.9, 128.5, 128.5, 134.8, 136.1, 138.2, 145.1, 160.4, 179.9. HRMS: calcd for $C_{15}H_{10}ClNO_2$, 271.6984; found, 271.0400.

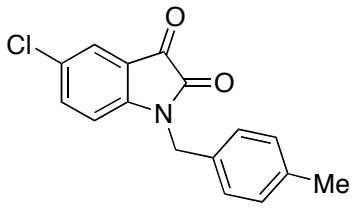

***N*-(4-Methylbenzyl)-5-chloroisatin** was prepared using general procedure B, (71%), orange solid, mp 310-312 °C. ^{1}H NMR (400 MHz, $CDCl_3$) δ 2.35 (3H, s), 4.94 (2H, s), 7.11 (4H, m, *J* = 7.5, 7.5, 1.5, 1.5 Hz), 7.75 (1H, dd, *J* = 7.5, 1.5 Hz), 7.79 (1H, s, *J* = 1.5 Hz), 7.94 (1H, d, *J* = 7.5 Hz). ^{13}C NMR (100 MHz, $CDCl_3$) δ 21.3, 47.6, 119.1, 124.7, 126.9, 128.1, 128.1, 128.8, 128.8, 133.1, 134.8, 136.1, 138.2, 145.1, 160.4, 179.9. HRMS: calcd for $C_{16}H_{12}ClNO_2$, 285.7250; found, 285.0557.

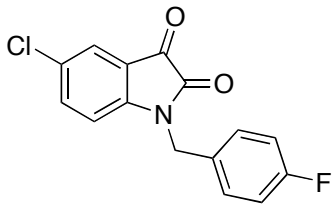

***N*-(4-Fluorobenzyl)-5-chloroisatin** was prepared using general procedure B, (78%), orange solid, mp 300-303 °C. ^{1}H NMR (400 MHz, $CDCl_3$) δ 4.94 (2H, s), 7.12 (2H, dd, *J* = 8.0, 7.5, 1.5 Hz), 7.39 (2H, dd, *J* = 7.5, 1.5, 5.0 Hz), 7.75 (1H, dd, *J* = 7.5, 1.5 Hz), 7.79 (1H, s, *J* = 1.5 Hz), 7.94 (1H, d, *J* = 7.5 Hz). ^{13}C NMR (100 MHz, $CDCl_3$) δ 47.6, 115.3, 115.3, 116.5, 117.6, 119.1, 124.0, 124.1, 124.7, 126.9, 128.5, 128.5, 131.7, 134.7, 138.4, 146.1, 160.4, 160.9, 179.9. HRMS: calcd for $C_{15}H_9ClNO_2$, 289.6889; found, 289.0306.

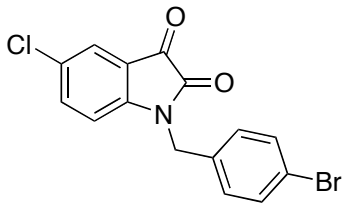

***N*-(4-Bromobenzyl)-5-chloroisatin** was prepared using general procedure B, (91%), orange solid, mp 358-360 °C.^{1}H NMR (400 MHz, $CDCl_3$) δ 4.94 (2H, s), 7.12 (2H, dd, *J* = 7.5, 1.5 Hz), 7.85 (2H, dd, *J* = 7.5, 1.5 Hz), 7.75 (1H, dd, *J* = 7.5, 1.5 Hz), 7.79 (1H, s, *J* = 1.5 Hz), 7.94 (1H, d, *J* = 7.5 Hz). ^{13}C NMR (100 MHz, $CDCl_3$) δ 47.6, 115.3, 119.1, 121.1, 124.0, 124.1, 124.7, 126.9, 129.1, 129.1, 131.4, 131.4, 134.7, 135.1, 138.2, 146.1, 160.4, 179.9. HRMS: calcd for $C_{15}H_9ClNO_2$, 350.5945; found, 350.9485.

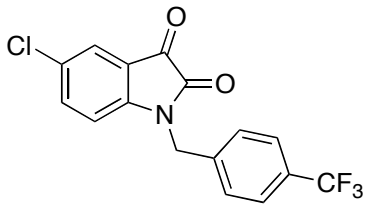

***N*-(4-(Trifluoro)methylbenzyl)-5-chloroisatin** was prepared using general procedure B, (89%), orange solid, mp 312-314 °C.^{1}H NMR (400 MHz, $CDCl_3$) δ 4.94 (2H, s), 7.16 (2H, dd, *J* = 7.5, 1.5 Hz), 7.50 (2H, dd, *J* = 7.5, 1.5 Hz), 7.75 (1H, dd, *J* = 7.5, 1.5 Hz), 7.79 (1H, s, *J* = 1.5 Hz), 7.94 (1H, d, *J* = 7.5 Hz). ^{13}C NMR (100 MHz, $CDCl_3$) δ 47.6, 119.1, 124.1, 124.7, 124.9, 124.9, 126.9, 128.5, 128.5, 129.0, 134.8, 138.2, 139.4, 146.2, 160.4, 179.9. HRMS: calcd for $C_{16}H_9ClF_3NO_2$, 339.6964; found, 339.0274.

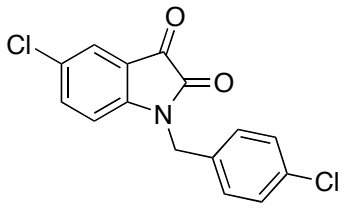

***N*-(4-Chlorobenzyl)-5-chloroisatin** was prepared using general procedure B, (51%), orange solid, mp 330-333 °C.^{1}H NMR (400 MHz, $CDCl_3$) δ 4.94 (2H, s), 7.32 (2H, dd, *J* = 7.5, 1.5 Hz), 7.37 (2H, dd, *J* = 7.5, 1.5, 5.0 Hz), 7.75 (1H, dd, *J* = 7.5, 1.5 Hz), 7.79 (1H, s, *J* = 1.5 Hz), 7.94 (1H, d, *J* = 7.5 Hz). ^{13}C NMR (100 MHz, $CDCl_3$) δ 47.6, 119.1, 124.7, 126.9, 128.6, 128.6, 129.3, 129.3, 132.3, 134.2, 134.8, 138.2, 146.2, 160.4, 179.9. HRMS: calcd for $C_{15}H_9Cl_2NO_2$, 306.1435; found, 305.0991.

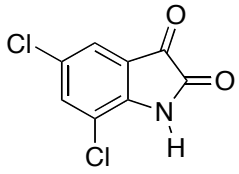

5,7-Dichloroisatin. A round-bottom flask was charged with chloral hydrate (0.55 g, 3.3 mmol), anhydrous Na_2SO_4 (3.41 g, 24 mmol), and EtOH/H_2O (v:v, 4 mL). The solution was acidified to a pH 1 with 6 N HCl. The reaction was stirred at 40 °C until the solution became clear. Solid 2,6-dichloroaniline (0.50 g, 3.0 mmol) and $NH_2OH{\cdot}HCl$ (0.70 g, 10 mmol) were added and the reaction was heated to 100 °C for 40 min. The reaction was cooled to rt and the isonitrosoacetanilide precipitate was formed. The precipitate was collected via filtration and dried under vacuum for 4 h. The dried precipitate was then

dissolved in concentrated H_2SO_4 (10 mL) and heated to 60 °C for 1 h. The reaction was cooled to rt and poured over cracked ice (20 mL) yielding an orange precipitate. The precipitate was collected via filtration and dried under vacuum overnight to give 0.56 g of the title compound as an orange solid (53%). mp 230 °C. ^{1}H NMR (400 MHz, $CDCl_3$) δ 7.67 (1H, s, *J* = 1.5 Hz), 8.0 (1H, s, br), 8.26 (1H, s, *J* = 1.5 Hz). ^{13}C NMR (100 MHz, $CDCl_3$) δ 120.5, 125.0, 132.4, 136.4, 137.9, 140.4, 159.3, 184.3. HRMS calcd for $C_9H_3Cl_2NO_2$, 216.0209; found 216.0265.

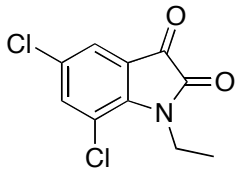

***N*-(Ethyl)-5,7-dichloroisatin** was prepared using general procedure B, (36%), orange solid, mp 242-246 °C.^{1}H NMR (400 MHz, $CDCl_3$) δ 1.32 (3H, t, *J* = 8.0 Hz), 4.28 (2H, q, *J* = 8.0 Hz), 7.67 (1H, s, *J* = 1.5 Hz), 8.29 (1H, s, *J* = 1.5 Hz). ^{13}C NMR (100 MHz, $CDCl_3$) δ 13.7, 42.0, 120.5, 125.0, 130.7, 136.4, 137.9, 140.4, 160.1, 179.9. HRMS: calcd for $C_{10}H_7Cl_2NO_2$, 244.0741; found, 244.0951.

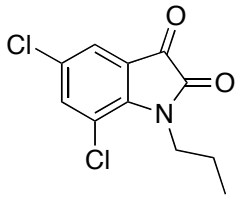

***N*-(1-Propyl)-5,7-dichloroisatin** was prepared using general procedure B, (20%), orange solid, mp 257-259 °C.^{1}H NMR (400 MHz, $CDCl_3$) δ 0.90 (3H, t, *J* = 8.0 Hz), 1.73 (2H, m, *J* = 7.1, 8.0 Hz), 4.28 (2H, t, *J* = 7.1 Hz), 7.67 (1H, s, *J* = 1.5 Hz), 8.29 (1H, s, *J* = 1.5 Hz). ^{13}C NMR (100 MHz, $CDCl_3$) δ 11.5, 20.5, 44.4, 120.5, 125.0, 130.7, 136.4, 137.9, 140.4, 160.1, 179.9. HRMS: calcd for $C_{11}H_9Cl_2NO_2$, 258.1007; found, 258.0044.

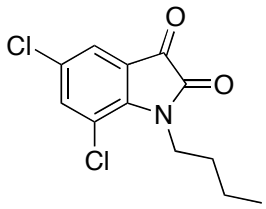

***N*-(1-Butyl)-5,7-dichloroisatin** was prepared using general procedure B, (12%), orange solid, mp 268-270 °C.^{1}H NMR (400 MHz, $CDCl_3$) δ 0.90 (3H, t, *J* = 8.0 Hz), 1.31 (2H, m, *J* = 7.1, 8.0 Hz), 1.52 (2H, m, *J* = 7.1, 7.1 Hz), 3.97 (2H, t, *J* = 7.1, 7.1 Hz), 7.67 (1H, s, *J* = 1.5 Hz), 8.29 (1H, s, *J* = 1.5 Hz). ^{13}C NMR (100 MHz, $CDCl_3$) δ 13.8, 20.1, 29.6, 41.9, 120.5, 125.0, 130.7, 136.4, 137.9, 140.4, 160.1, 179.9. HRMS: calcd for $C_{12}H_{11}Cl_2NO_2$, 272.1272; found, 272.0200.

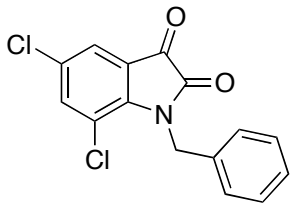

***N*-(Benzyl)-5,7-dichloroisatin** was prepared using general procedure B, (34%), orange solid, mp 330-332 °C.^{1}H NMR (400 MHz, $CDCl_3$) δ 4.94 (2H, s), 7.23 (2H, m, *J* = 1.5, 7.5, 7.5 Hz), 7.26 (1H, m, *J* = 7.5, 7.5, 1.5, 1.5 Hz), 7.33 (2H, m, 7.5, 7.5, 1.5 Hz), 7.67 (1H, s, *J* = 1.5 Hz), 8.29 (1H, s, *J* = 1.5 Hz). ^{13}C NMR (100 MHz, $CDCl_3$) δ 47.1, 120.5, 125.0, 126.7, 126.9, 126.9, 128.5, 128.5, 130.7, 136.1, 136.4, 137.9, 140.4, 160.4, 179.9. HRMS: calcd for $C_{15}H_9Cl_2NO_2$, 306.1435; found, 306.0044.

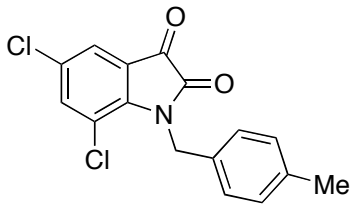

***N*-(4-Methylbenzyl)-5,7-dichloroisatin** was prepared using general procedure B, (53%), orange solid, mp 352-354 °C.^{1}H NMR (400 MHz, $CDCl_3$) δ 2.35 (3H, s), 4.94 (2H, s), 7.11 (4H, m, *J* = 7.5, 7.5, 1.5, 1.5 Hz), 7.67 (1H, s, *J* = 1.5 Hz), 8.29 (1H, s, *J* = 1.5 Hz). ^{13}C NMR (100 MHz, $CDCl_3$) δ 21.3, 47.1, 120.5, 125.0, 128.1, 128.1, 128.8, 128.8, 130.7, 133.1, 136.4, 136.4, 137.9, 140.4, 160.4, 179.9. HRMS: calcd for $C_{16}H_{11}Cl_2NO_2$, 319.0167; found, 319.0245.

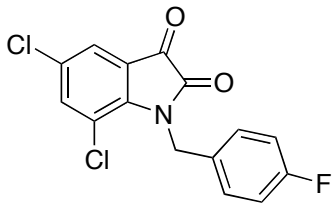

***N*-(4-Fluorobenzyl)-5,7-dichloroisatin** was prepared using general procedure B, (48%), orange solid, mp 340-342 °C.^{1}H NMR (400 MHz, $CDCl_3$) δ 4.94 (2H, s), 7.12 (2H, dd, *J* = 8.0, 7.5, 1.5 Hz), 7.39 (2H, dd, *J* = 7.5, 1.5, 5.0 Hz), 7.67 (1H, s, *J* = 1.5 Hz), 8.29 (1H, s, *J* = 1.5 Hz). ^{13}C NMR (100 MHz, $CDCl_3$) δ 47.1, 115.3, 115.3, 120.9, 125.0, 128.5, 128.5, 130.7, 131.7136.4, 137.9, 140.4, 160.4, 179.9. HRMS: calcd for $C_{15}H_8Cl_2FNO_2$, 322.9916; found, 323.0042.

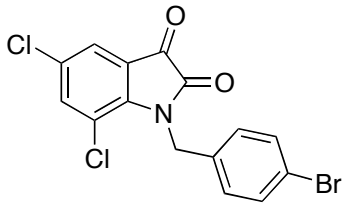

***N*-(4-Bromobenzyl)-5,7-dichloroisatin** was prepared using general procedure B, (41%), orange solid, mp 399-400 °C.^{1}H NMR (400 MHz, $CDCl_3$) δ 4.94 (2H, s), 7.12 (2H, dd, *J* = 7.5, 1.5 Hz), 7.85 (2H, dd, *J* = 7.5, 1.5 Hz), 7.67 (1H, s, *J* = 1.5 Hz), 8.29 (1H, s, *J* = 1.5 Hz). ^{13}C NMR (100 MHz, $CDCl_3$) δ 47.1, 120.5, 121.1, 125.0, 129.1, 129.1, 130.7, 131.4, 131.4, 135.1, 136.4, 137.9, 140.4, 160.4, 179.9. HRMS: calcd for $C_{15}H_8BrCl_2NO_2$, 382.9115; found, 382.9326.

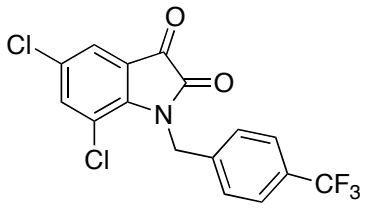

***N*-(4-(Trifluoro)methylbenzyl)-5,7-dichloroisatin** was prepared using general procedure B, (88%), orange solid, mp 356-359 °C.^{1}H NMR (400 MHz, $CDCl_3$) δ 4.94 (2H, s), 7.16 (2H, dd, *J* = 7.5, 1.5 Hz), 7.50 (2H, dd, *J* = 7.5, 1.5 Hz), 7.67 (1H, s, *J* = 1.5 Hz), 8.29 (1H, s, *J* = 1.5 Hz). ^{13}C NMR (100 MHz, $CDCl_3$) δ 47.1, 120.5, 124.1, 124.5, 124.5, 150.0, 128.9, 128.9, 129.0, 130.7, 136.4, 137.9, 139.4, 140.4, 160.5, 179.9. HRMS: calcd for $C_{16}H_8Cl_2F_3NO_2$, 372.9884; found, 373.0039.

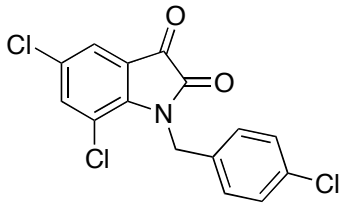

***N*-(4-Chlorobenzyl)-5,7-dichloroisatin** was prepared using general procedure B, (45%), orange solid, mp 369-371 °C.^{1}H NMR (400 MHz, $CDCl_3$) δ 4.94 (2H, s), 7.32 (2H, dd, *J* = 7.5, 1.5 Hz), 7.37 (2H, dd, *J* = 7.5, 1.5, 5.0 Hz), 7.67 (1H, s, *J* = 1.5 Hz), 8.29 (1H, s, *J* = 1.5 Hz). ^{13}C NMR (100 MHz, $CDCl_3$) δ 47.1, 120.5, 125.0, 128.6, 128.6, 129.3, 129.3, 130.7, 132.3, 134.2, 136.4, 137.9, 140.4, 160.4, 179.9. HRMS: calcd for $C_{15}H_8Cl_3NO_2$, 338.9621; found, 338.9847.

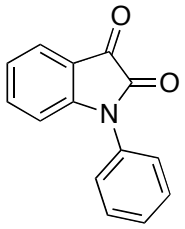

***N*-(Phenyl)-isatin** was prepared using general procedure C, (16%), orange solid, mp 243-246 °C. ^{1}H NMR (400 MHz, $CDCl_3$) δ 7.17 (1H, dd, *J* = 7.5, 7.5, 1.5, 1.5 Hz), 7.38 (1H, dd, *J* = 7.5, 7.5, 1.5 Hz), 7.43 (2H, m, *J* = 7.5, 7.5, 1.5, 1.5 Hz), 7.47 (2H, m, *J* = 7.5, 7.5, 1.5 Hz), 7.71 (1H, t, *J* = 7.5, 7.5 Hz), 8.05 (2H, dd, *J* = 7.5, 1.5 Hz). ^{13}C NMR (100 MHz, $CDCl_3$) δ 115.2, 121.9, 123.8, 126.4, 127.0, 127.0, 127.6, 129.6, 129.6, 135.4, 141.9, 144.4, 153.0, 184.3. HRMS: calcd for $C_{14}H_9NO_2$, 223.0633; found, 223.0978.

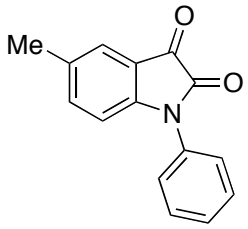

***N*-(Phenyl)-5-methylisatin** was prepared using general procedure C, (16%), orange solid, mp 256-258 °C. ^{1}H NMR (400 MHz, $CDCl_3$) δ 2.34 (3H, s), 7.19 (1H, dd, *J* = 7.5, 7.5, 1.5, 1.5 Hz), 7.43 (2H, m, *J* = 7.5, 7.5, 1.5, 1.5 Hz), 7.47 (2H, m, *J* = 7.5, 7.5, 1.5 Hz), 7.49 (1H, d, *J* = 1.5, 7.5 Hz), 7.58 (1H, s, *J* = 1.5 Hz), 7.88 (1H, d, *J* = 7.5 Hz). ^{13}C NMR (100 MHz, $CDCl_3$) δ21.3, 115.1, 119.5,

121.9, 124.7, 127.0, 127.0, 129.6, 129.6, 131.1, 135.7, 141.4, 141.9, 153.0, 184.3. HRMS: calcd for $C_{15}H_{11}NO_2$, 237.0790; found, 237.0991.

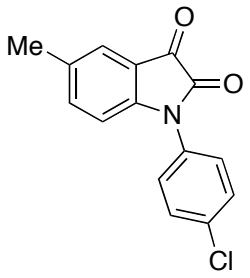

***N*-(4-Chlorophenyl)-5-methylisatin** was prepared using general procedure C, (25%), orange solid, mp 299-302 °C. ^{1}H NMR (400 MHz, $CDCl_3$) δ 2.34 (3H, s), 7.47 (2H, dd, *J* = 7.5, 7.5, 1.5,1.5 Hz), 7.49 (1H, d, *J* = 1.5, 7.5 Hz), 7.58 (1H, s, *J* = 1.5 Hz), 7.75 (2H, d, *J* = 7.5, 1.5 Hz), 7.88 (1H, d, *J* = 7.5 Hz). ^{13}C NMR (100 MHz, $CDCl_3$) δ 21.3, 115.1, 119.5, 124.7, 127.2, 129.7, 129.7, 131.3, 134.3, 134.3, 135.7, 140.0, 141.4, 153.0 184.3. HRMS: calcd for $C_{15}H_{10}ClNO_2$, 271.0400; found, 271.0739.

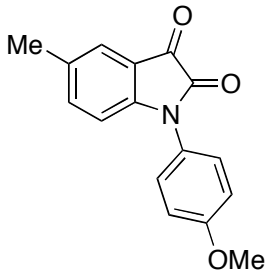

***N*-(4-Methoxyphenyl)-5-methylisatin** was prepared using general procedure C, (34%), orange solid, mp 300-302 °C. ^{1}H NMR (400 MHz, $CDCl_3$) δ 2.34 (3H, s), 3.83 (3H, s), 6.97 (2H, d, *J* = 7.5, 1.5 Hz), 7.17 (2H, d, *J* = 7.5, 1.5 Hz), 7.49 (1H, dd, *J* = 7.5, 1.5 Hz), 7.58 (1H, s, *J* = 1.5), 7.88 (1H, d, *J* = 7.5

Hz). ^{13}C NMR (100 MHz, $CDCl_3$) δ 21.3, 55.8, 115.1, 115.1, 115.2, 119.5, 124.7, 131.3, 133.7, 133.7, 132.2, 135.7, 141.4, 152.8, 153.0, 184.4. HRMS: calcd for $C_{16}H_{13}NO_3$, 267.0895; found, 267.0783.

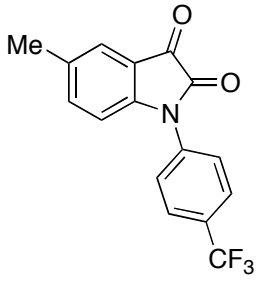

***N*-(4-(Trifluoro)methylphenyl)-5-methylisatin** was prepared using general procedure C, (5%), orange solid, mp 284-285 °C. ^{1}H NMR (400 MHz, $CDCl_3$) δ 2.34 (3H, s), 7.49 (1H, dd, *J* = 1.5, 7.5 Hz), 7.58 (1H, s *J* = 1.5 Hz), 7.60 (2H, dd, *J* = 7.5, 7.5, 1.5, 1.5 Hz), 7.74 (2H, dd, *J* = 7.5, 7.5, 1.5, 1.5 Hz), 7.88 (1H, d, *J* = 1.5 Hz). ^{13}C NMR (100 MHz, $CDCl_3$) δ 21.3, 115.1, 119.5, 124.1, 124.7, 126.0, 126.0, 130.8, 130.8, 131.3, 135.7, 141.4, 145.2, 153.0, 184.3. HRMS: calcd for $C_{16}H_{10}F_3NO_2$, 305.0664; found, 305.4378.

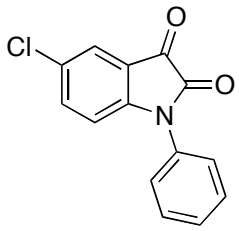

***N*-(Phenyl)-5-chloroisatin** was prepared using general procedure C, (32%), orange solid, mp 274-276 °C. ^{1}H NMR (400 MHz, $CDCl_3$) δ 7.19 (1H, dd, *J* = 7.5, 7.5, 1.5, 1.5 Hz), 7.43 (2H, m, *J* = 7.5, 7.5, 1.5, 1.5 Hz), 7.47 (2H, m, *J* =

7.5, 7.5, 1.5 Hz), 7.75 (1H, dd, *J* = 1.5, 7.5 Hz), 7.79 (1H, s, *J* = 1.5 Hz), 7.94 (1H, d, *J* = 7.5 Hz). ^{13}C NMR (100 MHz, $CDCl_3$) δ 116.6, 121.0, 121.9, 127.0, 127.0, 127.6, 129.6, 129.6, 132.1, 135.5, 141.9, 142.5, 153.0, 184.0. HRMS: calcd for $C_{14}H_8ClNO_3$, 257.0244; found, 257.0573.

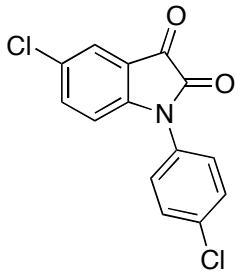

***N*-(4-Chlorophenyl)-5-chloroisatin** was prepared using general procedure C, (41%), orange solid, mp 316-318 °C. ^{1}H NMR (400 MHz, $CDCl_3$) δ 7.47 (2H, dd, *J* = 7.5, 7.5, 1.5,1.5 Hz), 7.75 (3H, m, *J* = 7.5, 7.5, 1.5, 1.5 Hz), 7.79 (1H, s, *J* = 1.5 Hz), 7.94 (1H, d, *J* = 7.5 Hz). ^{13}C NMR (100 MHz, $CDCl_3$) δ 116.6, 121.0, 127.2, 127.6, 129.7, 129.7, 132.1, 134.3, 134,3, 135.5, 140.0, 142.5, 153.0, 184.3. HRMS: calcd for $C_{14}H_7Cl_2NO_2$, 290.9854; found, 291.0023.

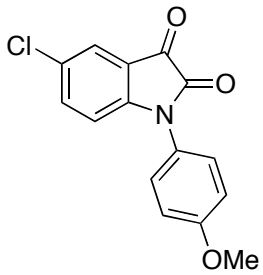

***N*-(4-Methoxyphenyl)-5-chloroisatin** was prepared using general procedure C, (23%), orange solid, mp 320-323 °C. ^{1}H NMR (400 MHz, $CDCl_3$) δ 3.83

(3H, s), 6.97 (2H, d, J = 7.5, 1.5 Hz), 7.17 (2H, d, J = 7.5, 1.5 Hz), 7.75 (1H, dd, J = 1.5, 7.5 Hz), 7.79 (1H, s, J = 1.5 Hz), 7.94 (1H, d, J = 7.5 Hz). ^{13}C NMR (100 MHz, $CDCl_3$) δ 55.8, 115.1, 115.1, 116.6, 121.0, 127.6, 133.7, 133.7, 134.2, 135.5, 142.5, 152.8, 153.0, 184.3. HRMS: calcd for $C_{15}H_{10}ClO_3$, 287.0349; found, 287.0591.

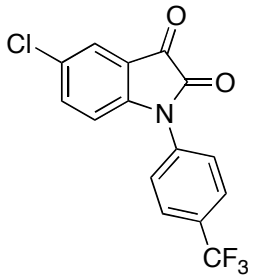

***N*-(4-(Trifluoro)methylphenyl)-5-chloroisatin** was prepared using general procedure C, (15%), orange solid, mp 302-304 °C. ^{1}H NMR (400 MHz, $CDCl_3$) δ 7.60 (2H, dd, J = 7.5, 7.5, 1.5, 1.5 Hz), 7.74 (2H, dd, J = 7.5, 7.5, 1.5, 1.5 Hz), 7.75 (1H, dd, J = 1.5, 7.5 Hz), 7.79 (1H, s, J = 1.5 Hz), 7.94 (1H, d, J = 7.5 Hz). ^{13}C NMR (100 MHz, $CDCl_3$) δ 116.6, 121.0, 124.1, 126.0, 126.0, 126.0, 127.6, 130.8, 130.8, 132.1, 135.5, 142.5, 145.2, 153.0, 184.3. HRMS: calcd for $C_{15}H_7ClF_3NO_2$, 325.0117; found, 325.0328.

References

(1) Brancale, A.; Silvestri, R. Indole, a Core Nucleus for Potent Inhibitors of Tubulin Polymerization. *Med. Res. Rev.* **2007**, *27*, 209-238.

(2) Downing, K.H. Structural Basis for the Interaction of Tubulin with Proteins and Drugs that Affect Microtubules Dynamics. *Ann. Rev. Cell Dev. Biol.* **2000**, *16*, 89-111.

(3) Mitchison, T.J.; Desai, A. Microtubule Polymerization Dynamics. *Ann. Rev. Cell Dev. Biol.* **1997**, *13*, 83-117.

(4) Downing, K.H.; Nogales, E. Tubulin and microtubule structure. *Curr. Opin. Cell. Biol.* **1998**, *10*, 16-22.

(5) Weisenberg, R.C.; Borisy, G.G.; Taylor, E.W. The Colchicine-Binding Protein of Mammalian Brain and its Relation to Microtubules. *Biochemistry* **1968**, *7*, 4466-4479.

(6) Burns, R.G. Alpha-, beta-, and gamma-tubulins: Sequence Comparisons and Structural Constraints. *Cell Motil. Cytoskelet.* **1991**, *20*, 181-189.

(7) Amos, L.; Klug, A. Arrangement of subunits in flagellar microtubules. *J. Cell Sci.* **1974**, *14*, 523-549.

(8) Evans, L.; Mitchison, T.; Kirschner, M. Influence of the Centrosome on the Structure of Nucleated Microtubules. *J. Cell Biol.* **1985**, *100*, 1185-1191.

(9) Raff, E.C.; Fackenthal, J.D.; Hutchen, J.A.; Hoyle, H.D.; Turner, F.R. Microtubule Architecture Specified by a Beta-Tubulin Isoform. *Science* **1997**, *275*, 70-73.

(10) Mitchison, T.J. Localization of an Exchangeable GTP Binding Site at the Plus End of Microtubules. *Science* **1993**, *261*, 1044-1047.

(11) Hirose, K.; Fan, J.; Amos, L.A. Re-examination of the Polarity of Microtubules and Sheets Decorated with Kinesin Motor Domain. *J. Mol. Biol.* **1995**, *251*, 329-333.

(12) Fan, J.; Griffiths, A.D.; Lockhart, A.; Cross, R.A.; Amos, L.A. Microtubule Minus Ends can be Labeled with a Phage Display Antibody Specific to Alpha-tubulin. *J. Mol. Biol.* **1996**, *259*, 325-330.

(13) David-Pfeuty, T.; Erickson, H.P.; Pantaloni, D. Guanosine Triphosphatase Activity of Tubulin Associated with Microtubule Assembly. *Proc. Natl. Acad. Sci USA* **1977**, *74*, 5372-5376.

(14) Mitchison, T.; Kirschner, M. Dynamic Instability of Microtubule Growth. *Nature* **1984**, *312*, 237-242.

(15) Margolis, R.L.; Wilson, L. Opposite End Assembly and Issue of Microtubules at Steady State *in Vitro*. *Cell* **1978**, *13*, 1-8.

(16) Jordan, M.A.; Wilson, L. Microtubules as a Target for Anticancer Drugs. *Nat. Rev. Cancer* **2004**, *4*, 253-265.

(17) Shaw, S.L.; Kamayar, R.; Ehrhardt, D.W. Sustained Microtubule Treadmilling in *Arabidopsis* Cortical Arrays. *Science* **2003**, *300*, 1715-1718.

(18) Chen, W.; Zhuang, D. Kinetochore Fibre Dynamics Outside the Context of the Spindle During Anaphase. *Nature Cell Biol.* **2004**, *6*, 227-231.

(19) Barron, D. M.; Kingston, D.; Chatterjee, S.K.; Ravindra, R.; Roof, R.; Baloglu, E.; Bane, S. A Fluorescence-based High-Throughput Assay for Antimicrotubule Drugs. *Anal. Biochem.* **2003**, *315*, 49-56.

(20) Hamel, E.; Covell, D.G. Classification of Anti-Mitotic Agents. *Curr. Med. Chem. Anticancer Ag.* **2002**, *2*, 19-53.

(21) Nogales, E.; Wold, S.G.; Khan, I.A.; Ludeuena, R.F.; Downing, K.H. Structure of Tubulin at 6.5A and Location of the Taxol-Binding Site. *Nature* **1995**, *375*, 424-427.

(22) Wilson, L.; Panda, D.; Jordan, M.A. Modulation of Microtubule Dynamics by Drugs: A Paradigm for the Actions of Cellular Regulators. *Cell Struct. Funct.* **1999**, *24*, 329-335.

(23) Bollag, D.M.; McQueney, P.A.; Zhu, J.; Hensens, O.; Koupal, L. Epothilones, A New Class of Microtubule-Stabilizing Agents with a Taxol-Like Mechanism of Action. *Cancer Res.* **1995**, *55*, 2325-2333.

(24) ter Haar, E.; Rosenkranz, H.S.; Hamel, E.; Day, B.W. Computational and Molecular Modeling Evaluation of the Structural Basis for Tubulin

Polymerization Inhibition by Colchicine Site Agents. *Bioorg. Med. Chem.* **1996**, *4*, 1659-1671.

(25) Lindel, T.; Jensen, P.R.; Fenical, W.; Long, B.H.; Casazza, A.M. Eleutherobin, a New Cytotoxin that Mimics Paclitaxel (Taxol) by Stabilizing Microtubules. *J. Am. Chem. Soc.* **1997**, *119*, 8744-8745.

(26) Uppuluri, S.; Knipling, L.; Sackett, D.L.; Wolff, J. Localization of the colchicine-binding site of tubulin. *Proc. Natl. Acad. Sci. USA* **1993**, *90*, 11598-11602.

(27) Rai, S.S.; Wolff, J. Localization of the Vinblastine-Binding Site of Beta-Tubulin. *J. Biol. Chem.* **1996**, *271*, 14707-14711.

(28) Jordan, M.A.; Margolis, R.L.; Himes, R.H.; Wilson, L. Identification of a Distinct Class of Vinblastine Binding Sites on Microtubules. *J. Mol. Biol.* **1986**, *187*, 61-73.

(29) Banwell, M.G.; Flynn, B.L.; Willis, A.C.; Hamel, E. Synthesis, X-Ray Crystal Structure and Tubulin-Binding Properties of a Benzofuran Analogue of the Potent Cytotoxic Agent Combretastatin A4. *J. Austr. Chem.* **1999**, *52*, 767-774.

(30) Cragg, G.M.; Newman, D.J. A Tale of Two Tumor Targets: Topoisomerase I and Tubulin. The Wall and Wani Contribution to Cancer Chemotherapy. *J. Nat. Prod.* **2004**, *67*, 232-244.

(31) Bonne, D.; Heusele, C.; Simon, C.; Pantaloni, D. 4',6-Diamidino-2-phenylindole, a Fluorescent Probe for Tubulin and Microtubules. *J. Biol. Chem.* **1985**, *260*, 2819-2825.

(32) da Silva, J.F.M.; Garden, S.J.; Pinto, A.C. The Chemistry of Isatins: a Review from 1975 to 1999. *J. Braz. Chem. Soc.* **2001**, *12*, 273-324.

(33) Bergman, J.; Lindstrom, J.O.; Tilstam, U. The Structure and Properties of Some Indolic Constituents in *Couroupita Guianensis* Aubl. *Tetrahedron* **1985**, *41*, 2879-2881.

(34) Yoshikawa, M.; Murakami, T.; Kishi, A.; Sakurama, T.; Matsuda, H.; Nomurea, M.; Matsuda, H.; Kubo, M. Novel Indoles, *O-Bisdesmoside*, *Calanthoside*. The Precursor Glycoside of Tryptanthrin, Indirubin, and Isatin, with Increasing Skin Blood Flow Promoting Effects from two Calanthe Species (Orchidaceae). *Chem. Pharm. Bull.* **1998**, *46*, 886-888.

(35) Kapadia, G.J.; Shukla, Y.N.; Basak, S.P.; Sokoloski, E.A.; Fales, H.M. The Melosatins-A Novel Class of Alkaloids from *Melochia Tomentosa*. *Tetrahedron* **1980**, *36*, 2441-2447.

(36) Grafe, U.; Radics , L.J. Isolation and Structure Elucidation of 6-(3'-Methylbuten-2'-yl) Isatin, and Unusual Metabolite from *Streptomyces Albus*. *J. Antibiotics* **1986**, *39*, 162-163.

(37) Marvel, C.S.; Hiers, G.S. Isatin. *Org. Syn. Coll.* **1941**, *1*, 327-329.

(38) Francotte, E.; Merenyi, R.; Vandenbulcke-Coyette, B.; Viehe, H.G. Nitrosoalkenes: Synthesis and Reactivity. *Helv. Chim. Acta* **1981**, *64*, 1208-1218.

(39) Kailia, N.; Janz, K.; Huang, A.; Moretto, A.; DeBernardo, S.; Bedard, P.W.; Tam, S.; Clerin, V.; Keith, J.C., Jr.; Tsao, D.H.H.; Sushkova, N.; Shaw, G.D.; Camphausen, R.T.; Schaub, R. G.; Wang, Q. 2-(4-Chlorobenzyl)-3-hydroxy-7,8,9,10-tetrahydrobenzo[*H*]quinoline-4-carboxylic Acid (PSI-697): Identification of a Clinical Candidate from the Quinoline Salicylic Acid Series of P-Selectin Antagonists. *J. Med. Chem.* **2007**, *50*, 40-64.

(40) Gassman, P.G.; Cue, B.W., Jr.; Luh, T.Y. A General Method for the Synthesis of Isatin. *J. Org. Chem.* **1977**, *42*, 1344-1348.

(41) Hewawasam, P.; Meanwell, N.A. A General Method for the Synthesis of Isatins: Preparation of Regiospecifically Functionalized Isatins from Anilines. *Tetrahedron Lett.* **1994**, *35*, 7303-7306.

(42) Igosheva, N.; Lorz, C.; O'Conner, E.; Glover, V.; Mehmet, H. Isatin, an endogenous monoamine oxidase inhibitor, taggers a dose- and time-dependent switch from apoptosis to necrosis in human neuroblastoma cells. *Neurochem. Int.* **2005**, *47*, 216-224.

(43) Chohan, Z.; Pervez, H.; Rauf, A.; Khan, K.M.; Supura, C.T. Isatin-derived Antibacterial and Antifungal Compounds and their Transition Metal Complexes. *J. Enz. Inhib. Med. Chem.* **2004**, *19*, 417-423.

(44) Natarnath, A.; Fan, Y.H.; Chen, H.; Guo, Y.; Iyasere, J.; Harbinski, F.; Christ, W.J.; Aktas, H.; Halperin, J.A. 3,3-Diaryl-1,3-dihydroindol-2-ones as Antiproliferatives Mediated by the Translation Initiation Inhibition. *J. Med. Chem.* **2004**, *47*, 1882-1885.

(45) Pandeya, S.N.; Smtha, S.; Jyoti, M.; Sridhar, S.K. Biological Activities of Isatin and its Derivatives. *Acta. Pharm.* **2005**, *55*, 27-46.

(46) Matheus, M.E.; Violante, F.; Garden, S.J.; Pinto, A.C.; Fernandes, P.D. Isatins inhibit Cyclooxygenase-2 and inducible Nitric Oxide Synthase in a mouse macrophage cell line. *Eur. J. Pharm.* **2007**, *556*, 200-206.

(47) Zhou, L.; Liu, Y.; Zhang, W.; Wei, P.; Huang, C.; Pei, J.; Yuan, Y.; Lai, L. Isatin Compounds as Noncovalent SARS Coronavirus 3C-like Protease Inhibitors. *J. Med. Chem.* **2006**, *49*, 3440-3443.

(48) Pirrung, M.C.; Pansare, S.V.; Das Sarma, K.; Keith, K.A.; Kern, E.R. Combinatorial Optimization of Isatin-B-Thiosemicarbazones as Anti-poxvirus Agents. *J. Med. Chem.* **2005**, *48*, 3045-3050.

(49) Konkel, M.K.; Lagu, B.; Boteju, L.W.; Jimenez, H.; Noble, S.; Walker M.W.; Chandrasena, G.; Blackburn, T.P.; Nikam, S.S.; Wright, J.L.; Korberg, B.E.; Gregory, T.; Pugsley, T.A.; Akunne, H.; Zoski, K.; Wise, L.D. 3-Arylimino-2-indolones Are Potent and Selective Galanin Gal3 Receptor Antagonists. *J. Med. Chem.* **2006**, *49,* 3557-3558.

(50) Kopka, K.; Faust, A.; Keul, P.; Wagner, S.; Breyholz, H.J.; Holtke, C.; Schober, O.; Schafers, M.; Levkau, B. 5-Pyrrolidinylsulfonyl Isatins as a Potential Tool for the Molecular Imaging of Caspases in Apoptosis. *J. Med. Chem.* **2006**, *49*, 6704-6715.

(51) Lisowski, V.; Robba, M.; Rault, S. Efficient Synthesis of Novel 3-(Het)arylanthranilic Acids via a Suzuki Cross-Coupling Reaction of 7-Iodoisatin with (Het)arylboronic Acids in Water. *J. Org. Chem.* **2000**, *65*, 4193-4194.

(52) Garden, S.J.; Torres, J.C.; da Silva, L.E.; Pinto, A.C.; Ferreira, A.A.; Silva, R.B. A modified Sandmeyer methodology and the Synthesis of (+/-)-Convolutamydine A. *Tetrahedron Lett.* **1997**, *38*, 1501-1504.

(53) Molander, G.A.; Biolatto, B. Palladium-Catalyzed Suzuki-Miyaura Cross-Coupling Reactions of Potassium Aryl- and Heteroaryltrifluoroborates. *J. Org. Chem.* **2003**, *68*, 4302-4314.

(54) Anderson, K.W.; Buchwald, S.L. General Catalysts for the Suzuki-Miyaura and Sonogashira Coupling Reactions of Aryl Chlorides and for the Coupling of Challenging Substrate Combinations in Water. *Ang. Chem. Int. Ed.* **2005**, *44*, 6173-6177.

(55) Bacher, G.; Nickel, B.; Emig, P.; Vanhoefer, U.; Seeber, S.; Shandra, A.; Klenner, T.; Beckers, T. D-24851, a Novel Synthetic Microtubule Inhibitor, exerts Curative Antitumoral Act *in Vivo*, Shows Efficacy toward Multidrug-

resistant Tumor cells, and Lacks Neurotoxicity. *Cancer Res.* **2001**, *61*, 392-399.

(56) De Martino, G.; Edler, M.C.; La Regina, G.; Coluccia, A.; Barbera, M.; Barrow, D.; Nicholson, R.I.; Chiosis, G.; Brancale, A.; Hamel, E.; Artico, M.; Silvestri, R. New Arylthioindoles: Potent Inhibitors of Tubulin Polymerization: Structure-Activity Relationships and Molecular Modeling Studies. *J. Med. Chem.* **2006**, *49*, 947-954.

(57) Garden, S.J.; Torres, J.C.; da Silva, L.E.; Pinto, A.C. A Convenient Methodology for the *N*-Alkylation of Isatin Compounds. *Syn. Comm.* **1998**, *28*, 1679-1689.

(58) Chan, D.M.T.; Monaco, K.L.; Wang, R.P.; Winter, M.P. New N- and O-Arylations with Phenylboronic Acids and Cupric Acetate. *Tetrahedron Lett.* **1998**, *39*, 2933-2936.

(59) Lam, P.Y.S.; Clark, C.G.; Saubern, S.; Adams, J.; Winters, M.P.; Chan, D.M.T.; Combs, A. New Aryl/Heteroaryl C-N Bond Cross-coupling Reactions via Arylboronic Acid/Cupric Acetate Arylation. *Tetrahedron Lett.* **1998**, *39*, 2941-2944.

(60) Klapars, A.; Antilla J.C.; Huang, X.; Buchwald, S.L. A General and Efficient Copper Catalyst for the Amidation of Aryl Halides and the *N*-Arylation of Nitrogen Heterocycles. *J. Am. Chem. Soc.* **2001**, *123*, 7727-7729.

(61) Klapars, A.; Huang, X.; Buchwald, S.L. A General and Efficient Copper Catalyst for the Amidation of Aryl Halides. *J. Am. Chem. Soc.* **2002**, *124*, 7421-7428.

(62) Antilla, J.C.; Klapars, A.; Buchwald, S.L. The Copper-Catalyzed *N*-Arylation of Indoles. *J. Am. Chem. Soc.* **2002**, *124*, 11684-11688.

(63) Mann, G.; Hartwig, J.F.; Driver, M.S.; Fernandez-Rivas, C. Palladium-Catalyzed C-N(sp_2) Bond Formation: *N*-Arylation of Aromatic and Unsaturated Nitrogen and the Reductive Elimination Chemistry of Palladium Azolyl and Methylenamido Complexes. *J. Am. Chem. Soc.* **1998**, *120*, 827-828.

(64) Skehan, P.; Storeng, R.; Scudiero, D.; Monks, A.; McMahon, J.; Vistica, D.; Warren, J.T.; Bokesch, H.; Kenney, S.; Boyd, M. New colorimetric cytotoxicity assay for anticancer-drug screening. *J. Natl. Cancer Inst.* **1990**, *82*, 1107-1112.

(65) Rubenstein, L.V.; Shoemaker, R.H.; Paull, K.D.; Simon, R.M.; Tosini, S.; Skehan, P.; Scudiero, D.A.; Monks, A.; Boyd, M.R. Comparison of in vitro anticancer-drug-screening data generated with a Tetrazolium assay versus a protein assay against a diverse panel of human tumor cell lines. *J. Natl. Cancer Inst.* **1990**, *82*, 1113-1118.